AD NUMBER

AD869324

NEW LIMITATION CHANGE

TO

Approved for public release, distribution unlimited

FROM

Distribution authorized to U.S. Gov't. agencies and their contractors; Administrative/Operational Use; Apr 1970. Other requests shall be referred to Director, Air Force Aero Propulsion Laboratory, Wright-Patterson AFB, OH 45433.

AUTHORITY

AFAPL ltr, 21 Sep 1971

AFAPL-TR-65-45
Part X

ROTOR-BEARING DYNAMICS DESIGN TECHNOLOGY

Part X: Feasibility Study of Electromagnetic Means to Improve the Stability of Rotor-Bearing Systems

T. Chiang

Mechanical Technology Incorporated

TECHNICAL REPORT AFAPL-TR-65-45, PART X

April 1970

Air Force Aero Propulsion Laboratory
Air Force Systems Command
Wright-Patterson Air Force Base, Ohio

116

NOTICE

When Government drawings, specifications, or other data are used for any purpose other than in connection with a definitely related Government procurement operation, the United States Government thereby incurs no responsibility nor any obligation whatsoever; and the fact that the government may have formulated, furnished, or in any way supplied the said drawings, specifications, or other data, is not to be regarded by implication or otherwise as in any manner licensing the holder or any other person or corporation, or conveying any rights or permission to manufacture, use, or sell any patented invention that may in any way be related thereto.

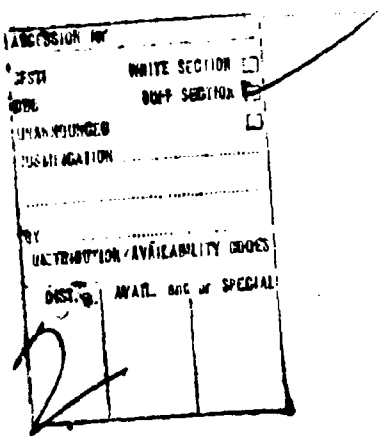

Copies of this report should not be returned unless return is required by security considerations, contractual obligations, or notice on a specific document.

FOREWORD

This report was prepared by Mechanical Technology Incorporated, 968 Albany-Shaker Road, Latham, New York 12110 under USAF Contract No. AF33(615)-3238. The contract was initiated under Project No. 3048, Task No. 304806. The work was administered under the direction of the Air Force Aero Propulsion Laboratory, with Mr. M. Robin Chaplan and Mr. Everett A. Lake (APFL) acting as project engineers.

The author wishes to express his gratitude to Professor L. P. Winsor, Department of Electrical Engineering, Rensselaer Polytechnic Institute, for his consultation in electromagnetic aspects, to Dr. C.H.T. Pan for useful suggestions and contributing the section on "Stabilization with Quadratic Damping", to Dr. J. H. Vohr for constructive discussions, to Mr. H. Clark and Mr. R. Sitts for consultation in electronic components, and to Mr. G. Moross for contributing the section on "Differentiator and Signal Splitter".

This report covers work conducted from 1 May 1967 to 1 September 1968.

This report was submitted in April, 1970.

This report is Part X of final documentation issued in multiple parts.

Publication of this report does not constitute Air Force approval of the report's findings or conclusions. It is published only for the exchange and stimulation of ideas.

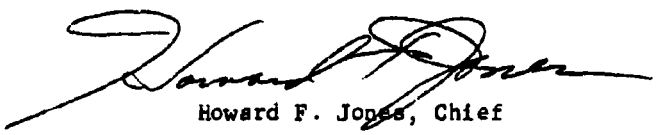

Howard F. Jones, Chief
Lubrication Branch
Fuel, Lubrication and Hazards Division
Air Force Aero Propulsion Laboratory

ABSTRACT

The feasibility of stabilizing gas bearing-rotor system by electromagnetic means was investigated analytically. Two devices appeared feasible, namely, a unidirectional device producing a magnetic force to load the bearing without increasing the rotor mass, and an active device producing a controlled electromagnetic force always opposing the motion of the shaft. A numerical example shows that the power loss from using either device together with plain journal bearings compares favorably with tilting-pad gas bearings.

TABLE OF CONTENTS

ILLUSTRATIONS

Figure

A	area [in^2]
A_c	area of magnetic core [in^2]
A_g	area of air gap [in^2]
A_k	area of conductor [cir. mil.]
A_1, B_1	defined in (13), [dimensionless]
$\bar{A}$	amplitude of current defined in (46), [amp]
B	magnetic flux density [line/in^2]
B_m	amplitude of flux density fluctuation [line/in^2]
C	radial bearing clearance [in]
D	bearing diameter [in]
d	magnet face width [in]
e_x, e_y	instantaneous bearing displacements [in]
e_{xo}	bearing steady-state displacement [in]
e_{xt}, e_{yt}	amplitudes of dynamic displacement [in]
E_1, E_2	defined in Appendix I, [dimensionless]
E	instantaneous electromotive force [volt]
E_1	voltage amplitude of amplifier output [volt]
E_{in}	induced e.m.f. [volt]
ΔE	voltage threshold of transistor [volt]
f	Ω/ω, [dimensionless]
F_m	magnetic force per air gap [lb]
$\bar{F}_o$	defined in (3), [dimensionless]
F_{xt}, F_{yt}	time-dependent forces [lb]
F_f	m.m.f. [amp. turn]

SYMBOLS

A	area [in^2]
A_c	area of magnetic core [in^2]
A_g	area of air gap [in^2]
A_k	area of conductor [cir. mil.]
A_1, B_1	defined in (13), [dimensionless]
$\bar{A}$	amplitude of current defined in (46), [amp]
B	magnetic flux density [line/in^2]
B_m	amplitude of flux density fluctuation [line/in^2]
C	radial bearing clearance [in]
D	bearing diameter [in]
d	magnet face width [in]
e_x, e_y	instantaneous bearing displacements [in]
e_{xo}	bearing steady-state displacement [in]
e_{xt}, e_{yt}	amplitudes of dynamic displacement [in]
E_1, E_2	defined in Appendix I, [dimensionless]
E	instantaneous electromotive force [volt]
E_1	voltage amplitude of amplifier output [volt]
E_{in}	induced e.m.f. [volt]
ΔE	voltage threshold of transistor [volt]
f	Ω/ω, [dimensionless]
F_m	magnetic force per air gap [lb]
$\bar{F}_o$	defined in (3), [dimensionless]
F_{xt}, F_{yt}	time-dependent forces [lb]
F_f	m.m.f. [amp. turn]

F, G	defined in Appendix I, [dimensionless]
H	dimensionless bearing gap, h/C
h	film thickness [in]
h_w	depth of coil winding [in], see Fig. 2
i	instantaneous electric current [amp]
i_o, i'	defined in (27), [amp]
k_m	static magnetic stiffness per air gap [lb/in]
K_h	hysteresis constant, units given in Section IV-5
L	bearing length [in]; inductance [Henry]
L_o, L'	defined in (25), [Henry]
ℓ_c	length of core [in] and rotor [in]
$\tilde{\ell}_c$	equivalent length of core and rotor [in]
ℓ_g	magnetic air gap [in]
ℓ_k	mean length of winding per turn [in]
ℓ_w, ℓ'_w	width and depth of coil winding [in], see Fig. 16
M	mass [lb]
m	dimensionless mass defined in (10)
m_c	dimensionless critical mass
N	number of turns
p	pressure [lb/in^2]
p_a	ambient pressure [lb/in^2]
P_h	hysteresis power loss [watts/lb]
q	number of laminations
R	resistance [Ohm]

t	time [sec]
v	velocity [in/sec]
U_{xx}, V_{xx}	defined in (5), [dimensionless]
U_{mgg}, V_{mgg}	dynamic magnetic stiffness and damping respectively in g-direction, [dimensionless]
U_{mxx}, V_{mxx}	dynamic magnetic stiffness and damping respectively in x-direction, [dimensionless]
w	magnet face depth [in]
W_{xo}, W_{yo}	dimensionless steady-state forces
W_{xt}, W_{yt}	dimensionless time-dependent forces
Z	bearing mechanical impedance, [dimensionless]
Z_r, Z_i	defined in (13), [dimensionless]
α	bearing attitude angle [rad]
β_m	defined in (55), [dimensionless]
γ	amplifier constant defined in (50), [volt sec/in]
ϵ_{xo}	e_{xo}/C, [dimensionless]
ϵ_{xt}	e_{xt}/C, [dimensionless]
ϵ_{yt}	e_{yt}/C, [dimensionless]
θ	polar coordinate [rad]
Λ	$\frac{6\mu\omega}{p_a}\left(\frac{D}{2C}\right)^2$, [dimensionless]
μ	viscosity [lb. sec/in^2]; magnetic permeability $\left[\frac{\text{lines/in}^2}{\text{Amp.turns/in}}\right]$
μ_o, μ_c	magnetic permeability of air and magnetic core $\left[\frac{\text{lines/in}^2}{\text{Amp.turns/in}}\right]$
τ	ωt [dimensionless]

φ	magnetic flux [lines]
ψ	phase angle defined in (47), [rad]
ω	journal angular velocity [rad/sec]
Ω	whirl angular velocity [rad/sec]

Subscripts

c	magnetic core
e	external
g	magnetic air gap
m	magnetic
o	steady-state
r	rotor
s	system
t	time-dependent
x,y,ξ,η	components along the respective directions (See Fig. 1)

Superscripts

dot	time derivative [1/sec]
prime	perturbation quantity
$\rightarrow$	vector quantity

SECTION I

INTRODUCTION

In high speed machinery applications, gas bearings have many advantages such as low friction, high stiffness, insensitivity to extreme thermal environment, radioactive "contamination", and so on. However, a gas bearing, because of its low damping characteristic, is susceptive to self-excited vibration which appears in the form of journal whirl motion. This motion, once started, will grow in amplitude until it either reaches a finite amplitude or results in solid contact between the journal and the bearing and thus causing bearing failure. Even the finite amplitude whirl may sometimes be considered unsatisfactory depending on the particular application and the magnitude of the whirl amplitude.

Shallow spiral grooves engraved on either the journal or the bearing surface were found both theoretically and experimentally to be effective in reducing whirl instability [Ref. 1, 2 and 3]*. However, in some range of operation, even a grooved bearing can have whirl instability. Tilting-pad gas bearings have been used successfully in many applications. Although tilting-pad gas bearings can be designed to operate quite stably, the designs are complex and power loss is high. Therefore, other means of improving the stability of journal bearings are desirable. One possibility is to utilize magnetic forces.

In the literature, magnetic suspension systems have been investigated [4] for space applications. The advantage of a magnetic bearing over a gas bearing is its ability to support load even in the absence of any lubricant. This makes magnetic bearings particularly suitable for suspension systems in high vacuum environment. However, magnetic bearings generally have much lower load capacity and stiffness than gas bearings.

In view of the above it appears logical to use the advantages of both a gas bearing and magnetic forces, i.e., we will use gas bearings to provide load capacity and stiffness, and magnetic forces, hopefully to supply the damping for bearing stabilization.

*Numbers in brackets refer to references at the end of this report.

The purpose of this effort, summarized by this report, was to investigate the feasibility of applying electromagnetic forces to stabilize gas journal bearings. Plain cylindrical journal bearings were chosen for investigation because of their simplicity in analysis and because they served the purpose of demonstrating how the whirl instability can be suppressed by electormagnetic devices.

SECTION II

THEORETICAL BACKGROUND

As stated in the Introduction, a plain cylindrical journal bearing was chosen for investigation. We shall briefly recapitulate in this section the theoretical background of stability analysis.

Following the approach [5], assume that the journal has a steady state displacement e_{xo} from concentric position. Let us choose the x-axis to coincide with the line connecting the concentric position and the displaced equilibrium position, and the y-axis, perpendicular to it (See Fig. 1). Let the journal have small oscillations with frequency Ω and amplitudes e_{xt} and e_{yt} in the x and y directions respectively. Then, from Fig. 1, it is illustrated that due to the steady-state displacement e_{xo}, there is a gap variation $e_{xo} \cos \theta$ (detailed derivation is provided on Pages 41 and 42 of Ref. [10]). Similarly, for the x and y oscillations, $e_{xt} \cos \Omega t$ and $e_{yt} \cos \Omega t$, the gap variations are $e_{xt} \cos \Omega t \cos \theta$ and $e_{yt} \cos \Omega t \sin \theta$ respectively. Thus, the dimensionless bearing gap can be expressed by

$$H = 1 - (\epsilon_{xo} + \epsilon_{xt} \cos f\omega t) \cos \theta - \epsilon_{yt} \cos f\omega t \sin \theta \qquad (1)$$

where $H = h/C$

$$\left.\begin{aligned} \epsilon_{xo} &= \frac{e_{xo}}{C} \\ \epsilon_{xt}, \epsilon_{yt} &= \frac{e_{xt}}{C}, \frac{e_{yt}}{C} \\ f &= \frac{\Omega}{\omega} \\ \omega &= \text{journal rotational speed} \end{aligned}\right\} \qquad (2)$$

Denote the steady-state lubricant pressure forces by F_{xo} and F_{yo}, and the dynamic forces by F_{xt} and F_{yt}. Then, by the linearized pH method, it is obtained from Ref. [5] that

$$\left.\begin{aligned} W_{xo} &= \frac{F_{xo}}{\pi\, DL\, p_a} = -\frac{1}{2}\ \epsilon_{xo}\, E_1 F \\ W_{yo} &= \frac{F_{yo}}{\pi\, DL\, p_a} = -\frac{1}{2}\ \epsilon_{xo}\, E_2 G \\ \overline{F}_o &= \sqrt{W^2_{xo} + W^2_{yo}} \end{aligned}\right\} \qquad (3)$$

and

$$\begin{bmatrix} W_{xt} \\ W_{yt} \end{bmatrix} = \frac{1}{\pi\, DL\, p_a} \begin{bmatrix} F_{xt} \\ F_{yt} \end{bmatrix} = -\begin{bmatrix} Z_{xx} & Z_{xy} \\ Z_{yx} & Z_{yy} \end{bmatrix} \begin{bmatrix} \epsilon_{xt} \\ \epsilon_{yt} \end{bmatrix} e^{\,if\omega t} \qquad (4)$$

where

$$Z_{xx} = U_{xx} + i\, V_{xx}, \text{ etc.} \qquad (5)$$

The Z matrix is the mechanical impedance of the bearing; the U_{xx} and V_{xx} are the direct dynamic stiffness and damping in the x direction, and Z_{xy} and Z_{yx} are cross-coupling terms. The Z's, E_1, E_2, F and G are given in [5] and listed in Appendix I for easy reference; they are functions of ϵ_{xo}, f and ω.

In general, the motion of the journal can be expressed by $e_{xt}\, e^{s\tau}$ and $e_{yt}\, e^{s\tau}$, with $\tau = \omega t$. At the onset of instability, s must be purely imaginary, because a real part would make an oscillatory motion either grow or decay depending on the sign of the real part. Thus, we set

$$s = i\, f_c \qquad (6)$$

where f_c is the critical speed ratio.

And the equations of motion are

$$M\, e_{xt}\, (i\, f_c \omega)^2\, e^{\,i\, f_c \tau} = F_{xt}$$

$$M\, e_{yt}\, (i\, f_c \omega)^2\, e\, i\, f_c \tau = F_{yt} \tag{7}$$

Using (4) and setting $f = f_c$, we have

$$-m\, f_c^2 \begin{bmatrix} e_{xt} \\ e_{yt} \end{bmatrix} e\, i\, f_c \tau = -\begin{bmatrix} Z_{xx} & Z_{xy} \\ Z_{yx} & Z_{yx} \end{bmatrix} \begin{bmatrix} e_{xt} \\ e_{yt} \end{bmatrix} e^{\,i\, f_c t} \tag{8}$$

which is readily reduced to

$$\begin{bmatrix} Z_{xx} - m\, f_c^2 & Z_{xy} \\ Z_{yx} & Z_{yy} - m\, f_c^2 \end{bmatrix} \begin{bmatrix} e_{xt} \\ e_{yt} \end{bmatrix} = 0 \tag{9}$$

where

$$m = \frac{MC\omega^2}{\pi D L p_a} \tag{10}$$

Since Eq. (9) is homogeneous, the determinant of the coefficient matrix must vanish. Thus,

$$V_{xx} + V_{yy} \pm Z_i = 0 \tag{11}$$

and

$$m_c = \frac{0.5\, (U_{xx} + U_{yy} \pm Z_r)}{f_c^2} \tag{12}$$

where

$$Z_1 + iZ_i = \sqrt{A_1 + i B_1}$$

$$A_1 = (U_{xx} - U_{yy})^2 - (V_{xx} - V_{yy})^2 + 4 (U_{xy} U_{yx} - V_{xy} V_{yx}) \tag{13}$$

$$B_1 = 4 (U_{xy} V_{yx} + U_{yx} V_{xy}) + 2 (U_{xx} - U_{yy}) (V_{xx} - V_{yy})$$

The U's and V's are functions of $\bar{f}$ as indicated in Appendix I and Ref [5]. For a given rotational speed ω and steady-state displacement ϵ_{xo}, Eq. (11) determines the critical speed ratio f_c and Eq. (12) determines the critical mass parameter m_c.

It is customary in stability analysis to define a threshold speed from the critical mass.

Threshold speed $$\sqrt{\frac{\omega}{p_a LD\pi}} \left(\frac{M_c C}{F_o / p_a LD\pi} \right)^{1/2} = \sqrt{\frac{m_c}{F_o}} \tag{12a}$$

The critical mass parameter and the threshold speed are the upper limits for stable operation of the bearing. The actual values should be designed to stay below their upper limits to have a stability margin.

SECTION VII

TWO FEASIBLE APPROACHES

In the last section, we have described that the stability of a journal bearing can be expressed by a critical speed and a critical mass. The mass of the rotor must be kept below the critical mass for a stable operation.

It is shown in Ref. 2 that an unloaded plain cylindrical journal bearing is always unstable because it has a zero critical mass. This situation is inevitable if a bearing is to be operated in a zero-g environment. One possible means to make the bearing stable is to apply a unidirectional magnetic force so that the bearing will be run at an eccentric rather than the concentric position. Detail consideration to this approach will be presented later in this section.

Although we can calculate for a loaded journal bearing (grooved or ungrooved) the critical mass for instability, in many cases, the critical mass turns out to be lower than the rotor mass and the system would be unstable. Therefore, it is desirable to devise means to increase the critical mass and thereby make the system more stable. One such device will be shown to be very effective in achieving the above purpose; it will be called an active electromagnetic device (See Fig. 8).

Electromagnetic Relationships

Let us first recapitulate some basic electromagnetic formulae. In an electromagnet, the magneto-motive force (m.m.f.) is equal to the ampere-turn of the winding,

$$F_f = Ni \tag{14}$$

Denote

A_g = air gap area perpendicular to magnetic flux, in^2
ℓ_g = length of air gap, in.
ℓ_k = mean length of winding per turn, in.
A_k = area of conductor, circular mils

ℓ_c = length of core, in

φ = magnetic flux, lines

B = flux density, line/in^2

F_i = m.m.f., amp-turns

N = number of turns

i = electric current, amp

F_m = magnetic force per air gap, lb.

The magnetic force per air gap is given by (pages 37 of Ref. 9)

$$F_m = \frac{B^2 A_g}{72 \times 10^6} \tag{15}$$

Consider a magnetic circuit with reluctances of two air gaps, a magnetic core and a rotor, connected in series. The total reluctance $\mathcal{R}$, is the sum of the reluctances in series. That is,

$$\mathcal{R} = \frac{\ell_g}{\mu_o A_g} + \frac{\ell_g}{\mu_o A_g} + \frac{\ell_c}{\mu_c A_c} + \frac{\ell_r}{\mu_r A_r}$$

where μ_o, μ_c and μ_r are the magnetic permeabilities of the air gap, the core and the rotor respectively. Because the total reluctance is usually dominated by that of the air gaps, it is convenient to write

$$\mathcal{R} = \frac{1}{\mu_o A_g} (2 \ell_g + \tilde{\ell}_c)$$

where

$$\tilde{\ell}_c = \ell_c \frac{\mu_o}{\mu_c} \frac{A_g}{A_c} + \ell_r \frac{\mu_o}{\mu_r} \frac{A_g}{A_r}$$

is the equivalent length of core-rotor reluctance. Soft magnetic materials with high magnetic permeability are available. The permeability of these materials is, in general, not constant. Suppose that we choose from Ref. 11,

the supermalloy (16% Fe, 79% Ni, 5% Mo); it has a permeability range of 55,000 to 300,000 Gauss/Oersted, or 140,000 ~ 700,000 lines/in^2/amp.turn/in. The saturation flux density for this cast alloy is 50,000 lines/in^2. As will be seen later, the actual flux density is designed below 40,000 lines/in^2.

Now, for the purpose of an order-of magnitude analysis, suppose that a high permeability material such as supermalloy is chosen for both the core and the rotor, we may assume

i) $\mu_c = \mu_r = 140{,}000$ line/in^2/amp.turn/in

and ii) that the "flux passage length" through both the core and the rotor is

$$\ell_c \frac{A_g}{A_c} + \ell_r \frac{A_g}{A_r} = 20 \text{ in.}$$

The permeability of air is $\mu_o = 1$ Gauss/Oersted $= 2.54$ line/amp.turn in. Assuming the air gap to be 0.01 in., then,

$$\frac{\ell_c}{2\ell_g} \approx \frac{20 \times 2.54}{140{,}000 \times 2 \times 0.01} \approx \frac{1}{56} << 1$$

Therefore, for this analysis, the combined reluctance of the core and the rotor can be neglected when compared to the reluctance of the two air gaps. The reluctance of the magnetic circuit is, therefore,

$$\mathcal{R} = \frac{1}{\mu_o A_g} (2\ell_g)$$

Using the above expression for the reluctance of a magnetic circuit and following the derivation shown on page 33 of Ref. 9, we obtain (instead of Eq. (14) on page 33 of Ref. 9) a relationship between flux density and m.m.f.,

$$Ni = 0.313 B (2\ell_g) = 0.626 B \ell_g \qquad (16)$$

Note that F_m given by Eq. (15) is the magnetic force produced by one (magnetic air) gap. The total magnetic force will obviously be $2F_m$. Since there are

two journal bearings - one at each end of the shaft - each bearing will be forced to carry a magnetic shaft loading of F_m in addition to other existing shaft loads.

1. A Device Producing a Unidirectional Magnetic Force

A schematic diagram of this device is shown in Fig. 2. The magnetic force is produced by a d-c electromagnet. Magnetic lines are emitted from one "leg" of the magnet (north pole) to the rotor and back into the other "leg" (south pole). The rotor and the magnet should, of course, be made of magnetically permeable material.

Under steady-state condition, the current in the winding is

$$i_o = \frac{E_o}{R} \tag{17}$$

where E_o = steady-state electric potential [volt]
R = resistance, [ohm]

Knowing i, one can easily calculate B from Eq. (16) and F_m from Eq. (15). Note that the magnetic force F_m is always an attractive force. A magnetic stiffness can be defined as the increment of magnetic repulsive force per unit decrement of the air gap.

$$k_m = \frac{d(-F_m)}{-d\ell_g} = \frac{dF_m}{d\ell_g} \tag{18}$$

Using Eqs. (15) and (16) and carrying out the differentiation, it is readily obtained that

$$k_m = -\frac{4F_m}{2\ell_g} \tag{19}$$

Note, first of all, that the magnetic stiffness is negative. This is an undesirable feature because the stiffness of the rotor-bearing system will be decreased by the amount $4F_m/2\ell_g$.

In order to keep the magnitude of k_m small, it is desirable to have a relatively large ℓ_g; this, of course, requires a proportionally large Ni to drive the same amount of magnetic flux through the air gap. It is to be noted that k_m is the static magnetic stiffness. Under dynamic condition (i.e., the gap has a sinusoidal variation with time), the situation is different. First of all, the electric current is no longer E/R. Let us choose a coordinate system ξ as shown in Fig. 1. Assume that the motion of the rotor in the ξ-direction be represented by $e_{\xi t} \cos \Omega t$ with $e_{\xi t}$ much smaller than ℓ_g. Then the air gap can be expressed by

$$\ell_g = \ell_{go} + \ell_g' \; ; \quad \ell_g' \ll \ell_{go} \tag{20}$$

where

$$\ell_g' = - e_{\xi t} \cos \Omega t \tag{21}$$

The inductance of the electric circuit is given by

$$L = N \frac{d\varphi}{di} 10^{-8} \text{ henry} \tag{22}$$

But,

$$\varphi = B A_g = \frac{Ni}{0.313(2\ell_g)} A_g$$

Thus,

$$L = N \frac{d\varphi}{di} 10^{-8} = 3.19 \times 10^{-8} \frac{N^2 A_g}{2\ell_g} \tag{23}$$

Note that L is time dependent. Therefore, instead of the usual current equation

$$L \frac{di}{dt} + R i = E_o$$

we should use

$$\frac{d}{dt}(Li) + R i = E_o \tag{24}$$

Using Equations (20) and (23), Eq. (24) can be linearized by neglecting quadratic and higher order effects of the air gap perturbation. First, Eq. (23) can be written as

$$L = L_o + L' \tag{25}$$

where

$$L_o = 3.19 \times 10^{-8} \frac{N^2 A_g}{2 \ell_{go}}$$

$$L' = \frac{\ell_g'}{\ell_{go}} L_o \tag{26}$$

Since the current is also varying with time, we can write

$$i = i_o + i' \tag{27}$$

where i_o is the steady-state current and i', the perturbation. Now Eq. (24) becomes

$$\frac{d}{dt} (L_o + L') (i_o + i') + R (i_o + i') = E_o \tag{28}$$

which can be separated into a steady-state equation,

$$R i_o = E_o \tag{29}$$

and a perturbation equation,

$$L_o \frac{di'}{dt} + i_o \frac{dL'}{dt} + R i' = 0 \tag{30}$$

Note that in Eq. (30), we have neglected $L' \frac{di'}{dt}$ and $i' \frac{dL'}{dt}$, because these two terms are small when compared respectively with the first two terms in Eq. (30), i.e. $L' \frac{di'}{dt} << L_o \frac{di'}{dt}$ and $i' \frac{dL'}{dt} << i_o \frac{dL'}{dt}$.

Equation (29) indicates that the steady-state current is $\frac{E_o}{R}$ which agrees with Eq. (17) and is obviously valid. Equation (30) is the equation for the perturbation current. Rearranging (30), we obtain

$$\frac{di'}{dt} + \frac{R}{L_o} i' = - i_o \frac{d}{dt} \left(\frac{L'}{L_o}\right) \tag{31}$$

Corresponding to a periodic perturbed motion of the rotor such that

$$\ell_g = \ell_{go} - e_{gt} \cos \Omega t$$

the solution of Eq. (31) is [Ref. 12]

$$i' = i_o \frac{e_g t}{\ell_{go}} \Omega \left[\frac{R/L_o}{\Omega^2 + (R/L_o)^2} \sin \Omega t - \frac{\Omega}{\Omega^2 + (R/L_o)^2} \cos \Omega t \right] + i'' \exp \left(- \frac{R}{L_o} t\right) \tag{32}$$

The transient term, which decays exponentially, depends on the precise initial condition; for instance, assuming $i' (t=0) = 0$, we have $i'' = i_o \frac{e_g t}{\ell_{go}} \times \frac{\Omega}{\Omega^2 + (R/L_o)^2}$. In any case, the time constant, L_o/R, in a typical design, would be very small as will be illustrated in a numerical example on pages 17 and 18.

From Eq. (16)

$$B = \frac{Ni}{0.626\, \ell_g} = \frac{N(i_o + i')}{0.626\, (\ell_{go} + \ell_g')} \tag{33}$$

$$= B_o \left(1 + \frac{i'}{i_o} - \frac{\ell_g'}{\ell_{go}} \right)$$

where

$$B_c = \frac{Ni_o}{0.626\, \ell_{go}} \tag{34}$$

Finally, we can compute F_m from Eq. (15) and by neglecting terms involving products of perturbation quantities,

$$F_m = \frac{B_o^2 A_g}{72\times10^6} \left(1 + 2\frac{i}{i_o} - 2\frac{\ell_g'}{\ell_{go}}\right)$$

Let $F_m = F_{mo} + F_m'$ (35)

Then,

$$F_{mo} = \frac{B_o^2 A_g}{72\times10^6} \tag{35a}$$

$$F_m' = F_{mo}\left(2\frac{i'}{i_o} - 2\frac{\ell_g'}{\ell_{go}}\right) \tag{35b}$$

Substituting Eqs. (21) and (32) into Eq. (35b) and assuming that the transient term has already become negligible, we obtain

$$F_m' = F_{mo}\, 2\frac{C}{\ell_{go}}\, \epsilon_{gt} \left[\frac{\Omega R/L_o}{\Omega^2 + (R/L_o)^2} \sin \Omega t - \frac{-(R/L_o)^2}{\Omega^2 + (R/L_o)^2} \cos \Omega t\right] \tag{36}$$

where $\epsilon_{gt} = \frac{e_{gt}}{C}$ = dynamic eccentricity ratio

C = radial bearing clearance

F_m' is the perturbation force due to a shaft oscillation, $-e_{gt} \cos \Omega t$. Thus, the in-phase and out-of-phase components of F_m' represent respectively the dynamic stiffness and damping induced magnetically.

In order to express the magnetic force in terms of stiffness and damping we write Eq. (4) in the $\xi\eta$ coordinates.

$$\frac{1}{\pi DL\, p_a}\begin{bmatrix}(F_{\xi t})_m\\(F_{\eta t})_m\end{bmatrix} = -\begin{bmatrix}Z_{m\xi\xi} & Z_{m\xi\eta}\\ Z_{m\eta\xi} & Z_{m\eta\eta}\end{bmatrix}\begin{bmatrix}\epsilon_{\xi t}\\ \epsilon_{\eta t}\end{bmatrix} e^{i\Omega t} \tag{37}$$

where $Z_{m\xi\xi} = U_{m\xi\xi} + i\, V_{m\xi\xi}$, etc. The subscript, m, indicates quantities due to magnetic forces. From Eq. (37) we have

$$\frac{(F_{\xi t})_m}{\pi DL\, p_a} = -\Big[\epsilon_{\xi t}\,(U_{m\xi\xi}\cos\Omega t - V_{m\xi\xi}\sin\Omega t + \epsilon_{\eta t}\,(U_{m\xi\eta}\cos\Omega t - V_{m\xi\eta}\sin\Omega t)\Big] \tag{38}$$

If we identify F'_m of Eq. (36) with $(F_{\xi t})_m$ of Eq. (38), and equate terms of like combinations of $\epsilon_{\xi t}$ cos Ωt etc., we obtain

$$\left.\begin{aligned} U_{m\xi\xi} &= -2\,\bar{F}_{mo}\,\frac{C}{\ell_{go}}\,\frac{1}{1+(\Omega L_o/R)^2}\\ V_{m\xi\xi} &= 2\,\bar{F}_{mo}\,\frac{C}{\ell_{go}}\,\frac{(\Omega L_o/R)^2}{1+(\Omega L_o/R)^2}\end{aligned}\right\} \tag{39}$$

where

$$\bar{F}_{mo} = \frac{F_{mo}}{\pi DL\, p_a} = \sqrt{W_{xo}^2 + W_{yo}^2}$$

In order to express the magnetic force in terms of stiffness and damping, we write Eq. (4) in the $\xi\eta$ coordinates.

$$\frac{1}{\pi DL\ p_a}\begin{bmatrix}(F_{\xi t})_m\\(F_{\eta t})_m\end{bmatrix} = -\begin{bmatrix}Z_{m\xi\xi} & Z_{m\xi\eta}\\ Z_{m\eta\xi} & Z_{m\eta\eta}\end{bmatrix}\begin{bmatrix}\epsilon_{\xi t}\\ \epsilon_{\eta t}\end{bmatrix} e^{i\Omega t} \tag{37}$$

where $Z_{m\xi\xi} = U_{m\xi\xi} + i\,V_{m\xi\xi}$, etc. The subscript, m, indicates quantities due to magnetic forces. From Eq. (37) we have

$$\frac{(F_{\xi t})_m}{\pi DL\ p_a} = -\Big[\epsilon_{\xi t}\,(U_{m\xi\xi}\cos\Omega t - V_{m\xi\xi}\sin\Omega t + \epsilon_{\eta t}\,(U_{m\xi\eta}\cos\Omega t - V_{m\xi\eta}\sin\Omega t)\Big] \tag{38}$$

If we identify F'_m of Eq. (36) with $(F_{\xi t})_m$ of Eq. (38), and equate terms of like combinations of $\epsilon_{\xi t}\cos\Omega t$ etc., we obtain

$$\left.\begin{aligned} U_{m\xi\xi} &= -2\,\bar{F}_{mo}\,\frac{C}{\ell_{go}}\,\frac{1}{1+(\Omega L_o/R)^2}\\ V_{m\xi\xi} &= 2\,\bar{F}_{mo}\,\frac{C}{\ell_{go}}\,\frac{(\Omega L_o/R)^2}{1+(\Omega L_o/R)^2}\end{aligned}\right\} \tag{39}$$

where

$$\bar{F}_{mo} = \frac{F_{mo}}{\pi DL\ p_a} = \sqrt{W_{xo}^2 + W_{yo}^2}$$

Observe that as $\Omega \to 0$ for $\Omega << R/L_o$, the magnetic dynamic stiffness approaches the steady-state stiffness as given by Eq. (19) except a constant factor due to non-dimensionalization, and the magnetic dynamic damping approaches to zero. Therefore, the quasi static results, as expected, agree with the static results obtained before.

Equation (39) indicates that the electromagnet aside from providing a loading on the bearing and a negative stiffness, yields a positive damping dynamically; both are inversely proportional to the magnetic gap. They are plotted against $\Omega L_o/R$ in Fig. 3. Since the damping helps to stabilize whereas the negative stiffness tends to destabilize, it is desirable to have large values of $V_{m\xi\xi}$ but keep the magnitude of $U_{m\xi\xi}$ small. In order to do so, the parameter $\Omega L_o/R$ should be designed to be greater than unity as can be seen from Fig 3.

Recall that ξ is the direction of magnetic loading. If the magnet face is designed to have a small wrap angle, so that the reluctance is not appreciably changed with a shaft motion in the η-direction, we have

$$U_{m\eta\eta} = V_{m\eta\eta} = C \tag{40}$$

All the cross-coupling terms are also zero.

Now we can express the magnetic dynamic stiffness and damping in the xy-coordinates.

$$\left.\begin{aligned} \{U_{mxx},\ V_{mxx}\} &= \{U_{m\xi\xi},\ V_{m\xi\xi}\}\cos^2\alpha \\ \{U_{myy},\ V_{myy}\} &= \{U_{m\xi\xi},\ V_{m\xi\xi}\}\sin^2\alpha \\ \{U_{mxy},\ V_{mxy}\} &= \{U_{m\xi\xi},\ V_{m\xi\xi}\}\sin\alpha\cos\alpha \\ &= \{U_{myx},\ V_{myx}\} \end{aligned}\right\} \tag{41}$$

The angle α is the angle of rotation from the $\xi\eta$-coordinates to the xy-coordinates as shown in Fig. 1

The dynamic stiffness and damping of the rotor-bearing system is equal to the sum of the corresponding terms of the bearing (U_{xx}, ...) and the electromagnet (U_{mxx}, ...).

$$(U_{xx})_s = U_{xx} + U_{mxx}$$

$$(U_{xy})_s = U_{xy} + U_{mxy}, \text{ etc.} \qquad (42)$$

where the subscript s indicates the system. Knowing the system dynamic stiffness and damping, the critical speed ratio and the critical mass can be calculated from Eqs. (11) and (12).

Example — Plain journal bearing in zero-g field.

Input

$D = 1$ in.

$p_a = 14.7$ psi

$\ell_{go} = 0.1$ in.

$C = 0.001$ in.

$\mu = 0.27 \times 10^{-8}$ lb sec/in^2

$\Lambda = 0.1$

$\epsilon_{xo} = 0.2$

$\frac{L}{D} = 1$

$A_g = 0.2$ in^2

$A_k = 1000$ cir. mil.

$\ell_k = 2.5$ in.

$i = 1$ amp

From $\Lambda = \frac{6 \mu \omega}{p_a} \left(\frac{D}{2C}\right)^2 = 0.1$

we calculate $\omega = 363$ rad/sec.

To displace this bearing to an eccentricity of $\epsilon_{xo} = 0.2$, we need a bearing force of, from Eq. (3),

$$W_{xo} = -0.696 \times 10^{-4}$$

$$W_{yo} = 0.24 \times 10^{-2}$$

$$\alpha = 88.3^{\circ}$$

Then $\bar{F}_{mo} = \sqrt{W_{xo}^2 + W_{yo}^2} = 0.0024$

which corresponds to a dimensional loading of $F_{mo} = \bar{F}_{mo} \cdot \pi DL\, p_a = 0.111$ lb.

From Eq. (15) and Eq. (16) we calculate

$$B = 6326 \text{ lines/in}^2$$

$$N = 392 \text{ turns}$$

The inductance is, from Eq. (26)

$$L_o = \frac{N^2 A_g}{2 \ell_{go}} 3.19 \times 10^{-8} = 0.496 \times 10^{-2} \text{ henry}$$

If copper is used for the coil winding, the resistance is

$$R = \frac{10.4N}{A_k} \frac{\ell_k}{12} = 0.85 \text{ ohm}$$

Thus, the transient time constant is

$$\frac{L_o}{R} = \frac{0.496 \times 10^{-2}}{0.85} = 0.00583 \text{ sec.}$$

and it would take only 0.027 sec. for the magnitude of the transient term in Eq. (32) to be reduced to 1/100 of its initial value.

To find the critical speed ratio f_c, we try various values of f until Eq. (11) is satisfied. We illustrate the procedure here by taking f = 0.4995 (which is actually the critical speed ratio). Then, U_{mgg} and V_{mgg} can be calculated from Eq. (39) and U_{mxx} etc., from Eq. (41).

$$U_{mxx} = -0.19 \times 10^{-7}$$
$$U_{mxy} = U_{myx} = -0.656 \times 10^{-6}$$
$$U_{myy} = -0.227 \times 10^{-4}$$
$$V_{mxx} = 0.201 \times 10^{-7}$$
$$V_{mxy} = V_{myx} = 0.695 \times 10^{-6}$$
$$V_{myy} = 0.24 \times 10^{-4}$$

Now the coefficients for the system can be calculated from Eq. (42) assuming U_{xx} and so on have already been calculated from Ref. [5].

$$(U_{xx})_s = 0.716 \times 10^{-3}$$
$$(U_{xy})_s = 0.120 \times 10^{-1}$$
$$(U_{yx})_s = -0.123 \times 10^{-1}$$
$$(U_{yy})_s = 0.664 \times 10^{-3}$$
$$(V_{xx})_s = 0.122 \times 10^{-1}$$
$$(V_{xy})_s = -0.693 \times 10^{-3}$$
$$(V_{yx})_s = 0.681 \times 10^{-3}$$
$$(V_{yy})_s = 0.120 \times 10^{-1}$$

From Eq. (13)

$$A_1 = -0.586 \times 10^{-3}$$
$$B_1 = 0.667 \times 10^{-4}$$
$$Z_r = -0.1374 \times 10^{-2}$$
$$Z_i = -0.2425 \times 10^{-1}$$

Substituting into Eq. (11), we have $(V_{xx}\, s + V_{yy})\, s + \Sigma_1 = 0.196 \times 10^{-8} \simeq 0$

Thus, the value of $f = 0.4995$ is indeed the critical speed ratio. The dimensionless critical mass is, from Eq. (12)

$$m_c = 0.108 \times 10^{-4}$$

Threshold speed = 0.067.

For a plain journal bearing with L/D = 1, C = 0.001 in. and $\epsilon_{xo} = 0.2$, the threshold speed is plotted against Λ for various values of ℓ_{go} in Fig. 4. It is seen that the threshold speed increases with ℓ_{go} in the small Λ region. When $\ell_{go} = \infty$, the stability curve becomes that of a gravitationally loaded bearing; the number of ampere-turns required to magnetically load the bearing is of course infinite (because $\ell_{go} = \infty$). For moderate and high Λ the magnetically loaded bearing is as good as the gravity-loaded bearing. Similar stability maps for $\epsilon_{xo} = 0.4$ and 0.6 are shown in Figs. 5 and 6, respectively. In Fig. 7 the number of turns, N is plotted against Λ for the same journal bearing at $\epsilon_{xo} = 0.6$; the electric current in the coil is assumed to be fixed at one amp.

2. An Active Electromagnetic Device

In an active electromagnetic device, the motion of the shaft is sensed by capacitance probes. (See Fig. 8). Since the whirl motion is two-dimensional, two probes are needed and should be placed 90 degrees from each other. The output of the sensing probes will be amplified, then sent from the amplifiers to the windings of the electromagnets placed around the shaft. The electrical system will be connected in such a way that the electromagnets always exert forces opposing the motion of the shaft. Since an electromagnet can only exert attractive forces on the shaft, two electromagnets are needed in the horizontal direction and two in the vertical direction. Therefore, a total of four electromagnets are required for the device. Figure 8 illustrates a schematic diagram of the device. It is seen that there are two independent, but identical subsystems - - one to control the x-motion, and the other to control the y-motion. Each

subsystem consists of one capacitance probe, one differentiator, one amplifier, one signal splitter and two electromagnets. It is necessary to investigate the characteristics of one subsystem only. Let the displacement in the x-direction be represented by

$$e_x = e_{xo} + e_{xt} \cos \Omega t \qquad (43)$$

where e_{xo} is the steady-state displacement determined by the loading and the bearing characteristics, and e_{xt} is the peak amplitude of the time dependent term. Because the loading may change either in magnitude or in direction or both, e_{xo} would change accordingly. But as far as improving the system stability is concerned, we have no direct interest in e_{xo}. As a matter of fact, it is desirable to sense only the time dependent part of the displacement, so that each time there is a new e_{xo} we do not have to readjust the system. However, a displacement probe can only read e_x. This is why a differentiator is needed; it differentiates with respect to time the output of the displacement probe. The input to the amplifier is, therefore, $\dot{e}_x$ or $- e_{xt} \Omega \sin \Omega t$. Finally, the signal splitter is to decide which electromagnet to energize with the output of the amplifier. Physically, it is clear that if $\dot{e}_x$ is negative, electromagnet ① should be energized, or electromagnet ③ if otherwise. A description on the differentiator and the signal splitter is given in Appendix II.

The output of the differentiator or the input to the amplifier is proportional to the shaft center velocity, $- e_{xt} \Omega \sin \Omega t$. Let the peak amplitude of the amplifier output be E_1.

If we assume the time lag introduced by the amplifier (as well as the probe and differentiator) is negligibly small, then the amplifier output potential can be represented by $E_1 \sin \Omega t$. In the sketch, one full cycle of $E_1 \sin \Omega t$ is shown. The positive portion (solid line) will be channelled to energize EM ① whereas the negative portion (dotted line) is to energize EM ③

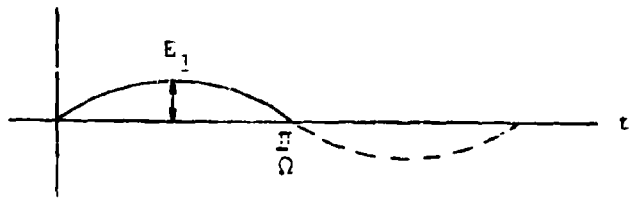

through the use of the signal splitter. The question then arises as to whether the current in the winding would be able to respond to the intermittent driving voltage illustrated in Fig. 9. To answer this, let us focus our attention on EM ① , it being a typical electromagnet in the system. The driving voltage on EM ① can be represented by

$$E = E_1 \sin \Omega t, \qquad 0 \leq t \leq \frac{\pi}{\Omega} \tag{44}$$

The electric current equation is, therefore

$$L \frac{di}{dt} + R\, i = E_1 \sin \Omega t, \quad 0 \leq t \leq \frac{\pi}{\Omega} \tag{45}$$

Suppose that the magnetic air gap is one order of magnitude larger than the bearing gap, so that the inductance L can be assumed to be constant. The solution of Eq. (45) is

$$i = \bar{A} \sin (\Omega t - \Psi) + \bar{A} \sin \Psi \exp \left(-\frac{R}{L} t\right) \tag{46}$$

where

$$\bar{A} = \frac{E_1/L}{\sqrt{\Omega^2 + (R/L)^2}} \quad ; \qquad \Psi = \tan^{-1} \left(\frac{\Omega L}{R}\right) \tag{47}$$

In order for the transient term in Eq. (46) to attenuate in a relatively short time interval, and in order for the phase angle Ψ to be small, the following inequality must be satisfied.

$$\frac{L}{R} << \frac{\pi}{\Omega} ; \text{ or } \frac{\Omega L}{R} << \pi \tag{48}$$

Only if inequality (48) is satisfied can the electric current in EM (1) be built up at no appreciable time lag and damped out quickly when it is not needed. This usually requires an additional external electric resistance in series with the winding. Having made R sufficiently large to satisfy (48), Eq. (47) can be approximated by

$$\bar{A} \approx E_1/R \; ; \quad \Psi \approx 0 \tag{49}$$

In some applications, the loss due to the addition of external electrical resistance can be quite large. It can even be the dominating loss in the bearing system. Therefore, it is interesting to consider the alternative of using a transistor in the circuit as shown in the following diagram for EM (1). Identical systems should be applied to the other three electromagnets.

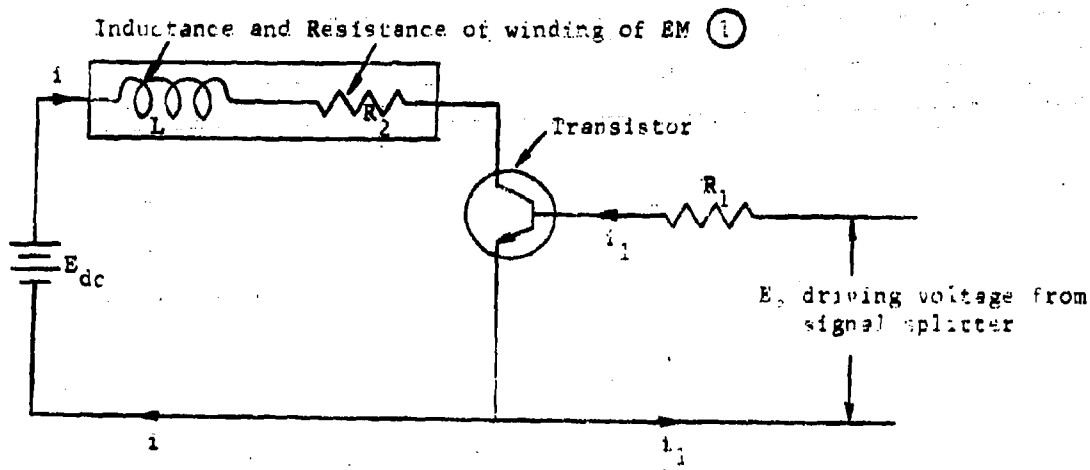

The driving voltage from signal splitter is connected to pass through a resistance R_1 which is much higher than the transistor resistance. This decreases the value of i_1 and causes it to be essentially in-phase with E. The actual current passing through the winding, i, can be on the order of 100 times the current i_1 controlling the transistor, i.e., the transistor acts as a current amplifier. Due to the operating characteristics of transistors the current i will be proportional to and in-phase with i_1 (and therefore in phase with E) and will be independent of the voltage drop L di/dt provided $E_{dc} \geq (L\, di/dt + R_2 i)_{max} - \Delta E$, where ΔE is the voltage threshold of the transistor. ΔE is typically 1 to 2 volts, and generally less than 5 volts. It is pointed out here that the power loss due to $i_1^2 R_1$ will be relatively low because i_1 is on the order of i/100.

Since the driving voltage on EM (1) and EM (3) is proportional to the shaft velocity, one can write by letting the proportionality constant be γ

$$E = \gamma \frac{de_x}{dt}$$

$$= -\gamma\Omega e_{xt} \sin \Omega t \qquad (50)$$

Eq. (43) has been used in deriving Eq. (50). Note that E is alternately applied to EM (1) in the interval $0 < \Omega t < \pi$, and to EM (3) in the interval $\pi < \Omega t < 2\pi$. The electric currents in the windings are again alternately

$$i = \frac{E}{R} = \frac{\gamma}{R} \frac{de_x}{dt} = -\frac{\gamma\Omega e_{xt}}{R} \sin \Omega t \qquad (51)$$

in the respective intervals. R is the external resistance in series with the winding, or in the case of the transistor circuit, an equivalent constant. The combined time-dependent magnetic force, $(F_{xt})_m$, of EM (1) and EM (3) by virtue of Eqs. (15), (16) and (51), can be expressed as

$$(F_{xt})_m = \frac{A_g}{72 \times 10^6} \left(\frac{N}{0.626\, \ell_g}\right)^2 \left(\frac{\gamma}{R}\right)^2 \left|\frac{de_x}{dt}\right| \frac{de_x}{dt} \qquad (52)$$

Employing an identical arrangement in the y-direction (see Fig. 8), EM (2) and EM (4) would similarly exert a time dependent magnetic force given by

$$(F_{yt})_m = \frac{A_g}{72 \times 10^6} \left(\frac{N}{0.626\, \ell_g}\right)^2 \left(\frac{\gamma}{R}\right)^2 \left|\frac{de_y}{dt}\right| \frac{de_y}{dt} \qquad (53)$$

Note that these forces, while acting to oppose the velocity of the shaft center, are proportional to the square of its magnitude. Therefore the stability analysis presented in Section III, in which various force components

are required to be linearly proportional to either the displacement or the velocity of the shaft center, can not be applied directly. In Appendix IV, a virtual damping criterion is derived showing that if magnetic forces such as those given in Eqs. (52) and (53) are employed to control the dynamic orbit of a shaft-bearing system, which would be otherwise unstable, an orbit of finite amplitude would develop. Thus, the type of magnetic forces discussed in this section does not stabilize the shaft in the absolute sense, but instead, it limits the amplitude of the shaft orbit. Equations (52) and (53) can be rewritten in a dimensionless form consistent with common conventions employed in bearing analysis, e.g. in Section II and Appendix IV.

$$\left.\begin{aligned} (W_{xt})_m &= \frac{(F_{xt})_m}{p_a \pi DL} = \beta_m \left|\frac{d\varepsilon_x}{d\tau}\right| \frac{d\varepsilon_x}{d\tau} \\ (W_{yt})_m &= \frac{(F_{yt})_m}{p_a \pi DL} = \beta_m \left|\frac{d\varepsilon_y}{d\tau}\right| \frac{d\varepsilon_y}{d\tau} \end{aligned}\right\} \qquad (54)$$

where

$$\beta_m = \left(\frac{C^2 \omega^2}{p_a \pi DL}\right) \left(\frac{A_g}{72 \times 10^6}\right) \left(\frac{N}{0.626\, \ell_g} \frac{\gamma}{R}\right)^2 \qquad (55)$$

Let us consider for example the case of an unloaded journal bearing. This bearing is inherently unstable. However, in the presence of stabilizing forces of the type considered here, the whirl motion is limited to an orbit of finite magnitude. As treated in detail in Appendix IV, the dominant component of such an orbit as estimated by a one-step iterative Fourier analysis would be a circle with the dimensionless radius

$$\frac{3\pi}{8} \left(\frac{U_{\perp 1} - V_{/\!/ 1}}{U_{/\!/ 1} + V_{\perp 1}}\right) \frac{m}{\beta_m} = \frac{3\pi}{8} \left(\frac{U_{\perp 1} - V_{/\!/ 1}}{f^2 \beta_m}\right)$$

where ($U_{//1}$, $V_{//1}$, $U_{\perp 1}$, $V_{\perp 1}$) are dynamically perturbed bearing forces (See Appendices I and IV) at the frequency ratio

$$f = \sqrt{\frac{U_{//1} + V_{\perp 1}}{m}}$$

which is approximately 0.5 regardless of the precise value of m. Thus, if the orbit size is to be limited to a designated amplitude, the required value of β_m must be sufficiently large.

For a loaded journal bearing, $\epsilon_{xo} \neq 0$, the analysis of Appendix IV would have to be extended to allow for the lack of symmetry between x and y directions. For a heuristic first approximation, one may replace Eqs. (54) by their dominant Fourier components evaluated at an acceptable upper bound of their amplitudes, say ϵ_1. In other words, one may make the approximation

$$\begin{bmatrix} (W_{xt})_m \\ (W_{yt})_m \end{bmatrix} = \begin{bmatrix} i\,V_{mxx} & 0 \\ 0 & i\,V_{myy} \end{bmatrix} \begin{bmatrix} \epsilon_{xt} \\ \epsilon_{yt} \end{bmatrix} \exp(ift) \qquad (56)$$

where

$$V_{mxx} = V_{myy} = \frac{8}{3\pi} f^2 \beta_m \epsilon_1 \qquad (57)$$

and then use the linear stability analysis according to Section II. For instance, with $\epsilon_1 = 0.1$, an unstable system (according to the linear stability analysis) would have an orbit with its dominant Fourier component larger than 0.1. Conversely, a stable system would have an orbit with its dominant Fourier component smaller than 0.1.

If one strives for a means to reduce the orbit size to an absolute zero, the magnetic damping must be not only phased to oppose the instantaneous velocity, but should also be made linearly proportional to its magnitude. Two ways of achieving linear magnetic dynamic damping appear possible. These are by means of a square root function generator and by means of d-c current bias. Each has serious shortcomings. In what follows below their operating principles will be

explained and shortcomings pointed out, so that one can, in the future, consider them as alternatives in a more rigorous trade-off study.

Square-Root Function Generator

A square-root function generator (SRFG) is a device which when fed by an input f (t) would produce an output $\sqrt{f(t)}$. If we connect in series one SRFG before each electromagnet, then it is quite obvious that the force produced will be proportional to e_{xt}. This will enable us to use the linear stability theory.

One such SRFG we have found is the General Electric Square-Root Convertor (GEMAC System HBK 8058B). According to the G.E. Brochure, it has the following characteristics:

Weight ---------- 5 pound net
Size ---------- 3" x 6" x 15"
Frequency Response ------ Down 3db at 3 Hz

The frequency response is definitely unsatisfactory because we are interested in the range of 100 Hz or higher.

D-C Current Bias

Apply a d-c bias electric current in the coil of each electromagnet. This bias current should be at least one order-of magnitude larger than the current driven by the amplifier. Let I_0 and I_1 denote respectively the d-c bias electric current and the current driven by the amplifier ($I_0 >> I_1$). Now the force produced by the electromagnet is proportional to $(I_0 + I_1)^2$.

Electromagnet Force $\sim (I_0 + I_1)^2 \approx I_0^2 + 2I_0I_1$. Note that we can neglect the I_1^2 term with the use of the d-c bias current. The force produced by the electromagnet is therefore proportional to I_1 and hence e_{xt}. Again, one can now use the linear stability theory.

However, this bias current gives rise to a steady magnetic force which in turn results in a negative stiffness. This negative stiffness should be appreciable because $I_0 >> I_{ac}$. Also the application of this bias current causes a large increase in power loss which will be discussed in the section entitled, Power Loss and Weight Penalties.

In summary, we do not recommend the use of either the SRFG or the d-c Bias Current just for the purpose of making the linear stability theory applicable. Due to the lack of knowledge about the influence of non-linear dynamic damping it is difficult to predict whether a linear or non-linear dynamic damping is more effective in suppressing whirl instability. But, qualitatively it is beyond doubt that the non-linear dynamic damping produced by the proposed active device will be effective in suppressing instabilities. In the following example, some preliminary stability results will be obtained by using the linear stability theory and Eq. (57)

EXAMPLE: Loaded Plain Journal Bearing

Input

D = 1 inch
C = 0.001 inch
μ = 0.27×10^{-8} lb.sec/in^2
Λ = 0.35
ϵ_{xo} = 0.2
L/D = 1

From the definition of Λ we calculate the journal speed ω = 1270 rad/sec. If we further specify the following:

Additional Input

N = 30 turns
i = 1 amp
R = 10 ohm (including external resistance)

$E_1 = 11.8$ volt

$A_g = 0.2$ in^2

$\ell_g = 0.01$ inch

In order to have $E_1 = 11.8$ volts, and suppose that the tolerable ϵ_1 is 0.118, then it is required that the amplifier can yield $\gamma \Omega C = 100$ volts. With the above input data, the magnetic dynamic damping can be readily calculated from (57).

$$V_{mxx} = V_{myy} = 0.0139$$

The values of V_{mxx} and V_{myy} can be easily increased by increasing the amplification ratio of the amplifier, γ.

Before we go any further, let us check if inequality (48) is satisfied. First of all, Ω is typically one half (or smaller) the journal speed, $\Omega = 635$ rad/sec. From Eq. (23), $L = 2.87 \times 10^{-4}$ henry

$$\frac{\Omega L}{R} = \frac{635 \times 2.87 \times 10^{-4}}{10} = 0.0182$$

which is indeed much smaller than π required by inequality (48).

The linear stability results for different values of magnetic dynamic damping are tabulated as follows:

V_{mxx} ($= V_{myy}$)	Dimensionless Threshold Speed (Eq. 12a)
0	0.286
0.005	0.375
0.010	0.575
0.015	0.891
0.020	1.373

At $V_{mxx} = 0.0139$, the threshold speed is 0.83, which is three times the value at $V_{mxx} = 0$.

SECTION IV

POWER LOSS AND WEIGHT PENALTIES

In the previous sections we have shown that both the device producing unidirectional magnetic force and the active device are capable of making a journal bearing more stable. It is then in order to estimate what penalties are associated with the use of either of the devices. One major penalty is of course the power loss associated with the electromagnetic system. The other major item is the weight penalty if the gas bearing is to be used in a space unit or any other circumstances where weight is an important consideration. It is illustrative to investigate an actual machine utilizing gas bearing suspension and compare the power loss with the machine power rating and the additional weight with the total weight of the machine.

Tilting-pad gas bearings supporting a 9 kw turboalternator were designed by MTI for NASA (under subcontract to Pratt-Whitney Aircraft). The bearings had been successfully operated for more than 1200 hours and they are still in operation. The bearing dimensions and generator characteristic data are listed below for easy reference.

9 kw , 4 pole, 400 Hz
Shaft diameter = 3-1/2 inch
Shaft speed = 12,000 rpm
Stator-rotor air gap = 20 mil
Rotor mass = 56 lb

1. Preliminary Design - Unidirectional Device

Suppose that we want to operate the unit described above in a zero-g environment with two plain journal gas bearings whose D = 3-1/2 inch, C = 0.001 inch and L/D = 1. One possible way to achieve a stable operation is utilizing the device producing a unidirectional magnetic force. In order to obtain a critical mass of 28 pounds which is half of the rotor mass (because there are two bearings), it is found that the bearings have to be loaded magnetically to an eccentricity of $\epsilon_{xo} = 0.41$, or $F_m = 82$ lb. Let the flux density be 40,000 line/in^2. Then, the area of the air gap needed is

$$A_g = \frac{F_m \times 72 \times 10^6}{B^2} = \frac{82 \times 72 \times 10^6}{(40,000)^2} = 3.69 \text{ in}^2$$

Design a cross-section of, say, w = 1-7/8 inch and d = 2 inch (see Fig. 13). Assume an air gap of ℓ_g = 0.01 inch, the ampere-turn required for the air gap is,

$$(Ni)_{gap} = (0.313 \text{ B } \ell_g)2 = 250 \text{ amp-turns}$$

Assume 50 amp-turns to take into account the drops in iron and leakage. Thus Ni = 250 + 50 = 300 amp-turns. Choose i = 1 amp, N = 300 turns and use #18 wire which has an o.d. of 0.04 inch and A_k = 1600 c.m. The cross-section of the coil winding would be 0.04 x 0.04 x 300 = 0.48 in^2. Allow an additional (see Fig. 13) 0.75 in^2 for insulation. Thus, to accommodate the coil winding and some margin we design a cross-sectional area of 2 in^2, so that

$$\ell_w = 2 \text{ inches}, \quad h_w = 1 \text{ inch}$$

2. Preliminary Design - Active Device

Design the system to be able to yield a maximum of V_{mxx} = 0.1 at ϵ_1 = 0.118. Then, the peak magnitude of magnetic time-dependent force is

$$(p_a \pi D L) V_{mxx} \epsilon_1$$

$$= (14.7 \times \pi \times 3.5 \times 3.5) 0.1 \times 0.118$$

$$= 6.67 \text{ pounds}$$

Assume B = 20,000 lines/in^2. Then, the area of the air gap is

$$A_g = \frac{6.67 (72 \times 10^6)}{20,000^2} = 1.2 \text{ in}^2$$

We can make the cross-section to be, say, w = 1.1 inch, d = 1.1 inch. Again assume an air gap of 0.01 inch. The ampere-turn required is 125. Allow an additional 25 amp-turns for leakage, etc. We need a peak total of 150 amp-turns. Choose a peak current of 1 amp and use #18 wire. N = 150 turns.

Since the ampere turn is one half of that of the unidirectional device, the cross-sectional area of the coil and insulation is also about half of it, $(0.48 + 0.75)/2 = 0.62$ in^2.

a. Loaded Bearing

If the bearing is loaded by its own weight, (28 lb/bearing) it will reach a static equilibrium position. For C = 0.001 inch, the bearing will develop this load capacity at $\epsilon_{xo} = 0.15$. The critical mass can be calculated to be three pounds. Since the critical mass is smaller than one half of the rotor mass, the bearing would be unstable. In order to make the rotor bearing system stable, the critical mass should be no less than 28 pounds. This can be achieved by using the active device. A plot of the critical mass against V_{mxx} is shown in Fig. 11. It is seen that a V_{mxx} of approximately 0.103 is needed to achieve a critical mass of 28 pounds.

In fact, if we design the bearing to have a larger clearance, the bearing would operate at a higher ϵ_{xo} but have smaller dynamic stiffness. As a result, the critical mass would have a lower value when $V_{mxx} = V_{myy} = 0$. However, it rises rather quickly with increasing magnetic damping as shown in Fig. 11. The following table summarizes the magnetic damping needed for various C to achieve a critical mass of 28 pounds.

C [in]	Λ	ϵ_{xo}	V_{mxx}	Critical Mass [lb]
0.0010	4.28	0.15	0.103	28
0.0015	1.90	0.24	0.092	28
0.0020	1.07	0.39	0.076	28

b. Unloaded Bearing

If the bearing is unloaded (e.g., in a zero-g environment), the critical mass is again plotted against V_{mxx} in Fig. 12. Note that the critical mass approaches zero when $V_{mxx} = 0$. This indicates the well-known fact that an unloaded journal bearing is always unstable. When $V_{mxx} = 0.1$, the critical mass becomes as high as 252.6 pounds. In the following we again summarize

the dynamic magnetic damping, V_{mxx}, needed for various C to achieve a critical mass of 28 pounds at zero eccentricity.

C [in]	V_{mxx}	Critical Mass [lb]
0.0010	0.109	28
0.0015	0.096	28
0.0020	0.077	28

It is therefore recommended to design the bearing at C = 0.002 inch, if the active device is to be used. To operate stably, it would need $V_{mxx} = V_{myy} = 0.076$ when it is loaded, $V_{mxx} = V_{myy} = 0.077$ when it is not loaded. For subsequent calculations, 0.08 will be used for the value of V_{mxx}. In Section IV-7, it will be seen that larger clearance would result in lower bearing frictional loss although the eccentricity will be higher.

3. Eddy Current Loss

The magnetic flux while passing through the shaft are cut by the rotation of the shaft and thus generating e.m.f. This e.m.f. will produce eddy-current and dissipate in the form of heat. In the following we will make an estimate of this eddy-current loss.

Magnetic flux will complete its path from one air gap through the shaft, the other air gap and back into the magnet. It will penetrate the entire depth of the shaft in a three-dimensional fashion which will be affected by the ratio of the magnet dimensions to the shaft diameter, the variation in permeability due to change in B, and the presence of eddy-current in the shaft.

While an actual analysis for the flux distribution is rather complicated, we assume for a first approximation, that the flux is flowing uniformly in a channel inside the shaft. The channel penetrates to depth d and width w in the shaft (i.e., the same dimensions as the outer core) as shown in Fig. 13. If the rotation of the shaft is as shown in Fig. 13, and the flux direction is to the right as shown, then the e.m.f. generated is radial in the central region and axial near the gap according to

$$d\vec{E}_{in} = (\vec{v} \times \vec{B}\ d\ell)\ 10^{-8} \qquad (58)$$

A current (eddy-current) is produced because of the induced e.m.f. and is in the same direction as E_{in}. A force proportional to the product of E_{in} and the current, acts in a direction to oppose the shaft motion. Hence, there is a drag, and eddy-current loss must be supplied mechanically by the shaft.

Let us focus our attention in the central region where the flux is toward the right and E_{in} is in the radial direction. The magnitude of the velocity is $v = \omega r$ and $d\ell = dr$ where ω is the rotating speed of the shaft and r the radial coordinate. Using the above and integrating (58) we have

$$E_{in} = B\,\omega \int_{\frac{D}{2}-d}^{\frac{D}{2}} r\,dr \times 10^{-8}$$

$$= \frac{1}{2} B\,\omega\,(Dd - d^2) \times 10^{-8}$$

Substituting values from the preliminary design

$B = 40{,}000$ lines/in^2

$\omega = 12000$ rpm $= 1255$ rad/sec

$D = 3.5$ inches

$d = 2$ inch

$$E_{in} = \frac{1}{2} \times 40{,}000 \times 1255\,(7 - 4) \times 10^{-8}$$

$= 0.756$ volts.

In order to calculate the eddy-current loss due to this induced voltage, it is necessary to estimate the electrical resistance of the current path. Assume that current is flowing over an area of cross section equal to the length and width of the magnet. Thus,

Area of cross section $= (\ell_w + d)\,w$

Length of current path $= d$

The electrical resistance of the induction path = $23.6 \times 10^{-6} \frac{d}{(\ell_w + d)w}$

$= 23.6 \times 10^{-6} \times \frac{2}{(2+2)1.88} = 6.27 \times 10^{-6}$ ohm if the shaft is made of supermalloy which has a resistivity of 23.6×10^{-6} ohm per inch length per square inch cross section. (See Page 5-180 of Ref. 14). Since electrical current will return through some path in the shaft, we assume that the total resistance is twice the value calculated above

$R = 12.5 \times 10^{-6}$ ohm. Eddy-current power loss $= \frac{E_{in}^2}{R} = \frac{0.756^2}{12.5 \times 10^{-6}} = 45.6 \times 10^3$ watts = 45.6 kw.

Thus, the estimated eddy-current power loss is about 5 times greater than the power rating of the turboalternator. Whatever the assumptions that are made regarding the flux distribution and current path etc., it is obvious that the eddy-current losses will be prohibitive at the speed and flux density specified.

If we use the active device instead, the eddy-current loss is then estimated to be 4 kw which is still very high.

A common practice in electrical machinery design to reduce eddy-current loss is by lamination, but it appears very difficult to laminate a shaft. We therefore propose to mount a laminated disk onto the shaft as shown in Figs. 14 and 15. Note that the electromagnets in Figs. 14 and 15 have been oriented in such a way that the induced e.m.f. is always perpendicular to the laminations. The laminated disk and the shaft are separated by a ring made of nonmagnetic, nonconducting material such as ceramic. It is seen that the induced e.m.f. is now only in the regions near the gaps. Suppose that there are q laminations. The induced e.m.f. and electrical resistance in each lamination are E_{in}/q and qR, respectively. The total eddy-current loss is clearly

$$q \frac{(E_{in}/q)^2}{q\,R} \quad \text{or} \quad \frac{1}{q^2} \frac{E_{in}^2}{R}$$

Thus, the eddy-current loss being proportional to the inverse square of q, can be very effectively reduced to a tolerable level by the addition of a laminated disk. A 0.02 inch thickness lamination is quite common. It will be seen later that the disk thickness is designed to be four inches for the unidirectional device and one inch for the active device.

Thus,

$$q = \frac{4}{0.02} = 200 \text{ laminations for the unidirectional device}$$

$$q = \frac{1}{0.02} = 50 \text{ laminations for the active device}$$

$$\text{Eddy-current loss} = \frac{45{,}600 \text{ watts}}{q^2} = \frac{45{,}600}{200^2}$$

$$= 1.1 \text{ watts for the unidirectional device}$$

$$\text{Eddy-current loss} = \frac{4000 \text{ watts}}{q^2} = \frac{4000}{50^2}$$

$$= 1.6 \text{ watts for the active device}$$

4. Proposed Design

Since it is always desirable to have the magnetic force concentrating at a particular radial direction rather than over a wide area, a better magnet design is shown in Fig. 16 in which the spacing between the pole pieces is reduced. Data of the improved designs for the magnet and the laminated disk are tabulated in the following. The subsequent estimates on power losses and weight penalty are based on this configuration.

	Unidirectional Device	Active Device
Laminated Disk Thickness	4 inches	1 inch
O.D.	6 inches	6 inches
I.D.	4 inches	4 inches
Magnet Face Width, d	0.92 inch	1.1 inch
Magnet Face Depth, w	4 inches	1.1 inch
Coil Cross-sectional Area	1.25 in^2	0.62 in^2
ℓ_w	1.25 inch	1 inch
ℓ'_w	1 inch	0.62 inch
Number of Magnets Needed	1	4

5. Hysteresis Loss

The hysteresis loss is given by (Ref. 6)

$$P_h = K_h f B_m^{1.6} \quad [\text{watt/lb}]$$

where f is the frequency in Hz, B_m is the maximum flux density in lines/in^2, and K_h is a material constant (which for the units stated above is 4×10^{-13} for supermalloy, Ref. 13, page 513).

In the device producing a unidirectional magnetic force, the flux density, according to the preliminary design is 40,000 lines/in^2. The flux fluxuation is due to shaft rotation, so that B_m = 40,000 lines/in^2 and f = 200 cps. In the active device, B_m is 20,000 lines/in^2 and the frequency f is 100 cps. if we assume a half-frequency whirl motion. Thus, the hysteresis losses are, using supermalloy as the magnetic material,

$$P_h = 4 \times 10^{-13} \times 100 \times 20{,}000^{1.6} = 0.0003 \text{ watts/lb}$$

for the active device, and

$$P_h = 4 \times 10^{-13} \times 200 \times 40{,}000^{1.6} = 0.0018 \text{ watts/lb}$$

for the unidirectional device.

The elements having magnetic flux fluctuation are the laminated disk and magnet cores in the active device, the laminated disk in the unidirectional device. As shown in Section IV-9, the weight of these elements is 4.98 + 4 x 2.92 = 16.7 lb. for the active device, and 19.9 lb. for the unidirectional device. Thus, the hysteresis loss is

0.0003 x 16.7 = 0.005 watts for the active device and
0.0018 x 19.9 = 0.036 watts for the unidirectional device

6. Copper Loss

a. Unidirectional Device

Mean length of one turn = $(w + \ell'_w + d + \ell'_w)2$ = (4 + 1 + 0.92 + 1)2
= 13.8 in.

Total length = 300 x 13.8 = 4130 inches = 344 feet
Area of #18 copper wire = 1600 c.m.

$$R = \frac{10.7 \times 3.44}{1600} = 2.3 \text{ ohm}$$

i = current = 1 amp
Power loss = i^2R = 2.3 watts

For each bearing, the copper loss is $\frac{2.3}{2}$ = 1.15 watts/bearing.

b. Active Device

Mean length of one turn = $(w + \ell'_w + d + \ell'_w)2$ = (1.1 + 0.62 + 1.1 + 0.62)2 = 6.88 in.

Total length = 150 x 6.88 = 1030 inches = 86 feet
Area of #18 copper wire = 1600 c.m.

$$R = \frac{10.7 \times 86}{1600} = 0.575 \text{ ohm}$$

As indicated before, an external resistance is often necessary in order to make the circuit resistive rather than inductive. The inductance is by Eq. (23),

$$L = 3.19 \times 10^{-8} \frac{N^2 A_g}{2 \ell_g}$$

$$= 3.19 \times 10^{-8} \frac{150^2 \times 1.21}{2 \times 0.01} = 4.35 \times 10^{-2} \text{ henry}$$

Assume that the whirl speed is half the shaft speed, then

$$\Omega = \frac{1}{2} 1225 = 628 \text{ rad/sec}$$

$$\Omega L = 628 \times 4.35 \times 10^{-2} = 27.3 \text{ ohm}$$

If we add an external resistance to make a total resistance of $R_e = 140$ ohm, then $\Omega L/R_e = 0.195$ which is one order of magnitude smaller than 1. With a peak current of 1 amp, the current in EM (1) is, from Eqs. (46) and (49), $i = I_{max} \sin \Omega t$.

Thus,

$$\text{copper loss in EM (1)} = \frac{1}{2\pi} \int_0^{\pi} i^2 R_e \, d(\Omega t) = \frac{R_e}{2\pi} \int_0^{\pi} I_{max}^2 \sin^2 \Omega t \, d(\Omega t)$$

$$= \frac{I_{max}^2 R_e}{4} = \frac{140}{4} = 35 \text{ watt}$$

Since there are four electromagnets in the active device, total copper loss = 4 x 35 = 140 watts. And because there are two bearings, the copper loss per bearing is 140/2 = 70 watts/bearing.

As indicated on Page 23, one can use a transistor circuit instead of adding external resistance, to achieve the same purpose. From the calculations on pages 39 and 40, we have

$L = 4.35 \times 10^{-2}$ henry

R = Resistance of coil winding

= 0.575 ohm

$i = I_{max} \sin \Omega t$

$I_{max} = 1$ amp.

Thus, we calculate

$$\left(L \frac{di}{dt} + Ri\right)_{max} = \left(L I_{max} \Omega \cos \Omega t + R I_{max} \sin \Omega t\right)_{max}$$

$$= \left(4.35 \times 10^{-2} \times 628 \cos \Omega t + 0.575 \sin \Omega t\right)_{max}$$

$$= \left(27.3 \cos \Omega t + 0.575 \sin \Omega t\right)_{max}$$

$$= 27.3 \text{ volt}$$

If we allow conservatively 5 volts for the transistor threshold voltage, then from the formula on Page 23

$$E_{dc} = \left(L \frac{di}{dt} + Ri\right)_{max} + \Delta E$$

$$= 27.3 + 5 = 32.3 \text{ volt minimum}$$

The transistor circuit loss in one of the electromagnets, say, EM (1) , is then

$$\frac{1}{2\pi} \int_0^{\pi} i E_{dc} \, d(\Omega t) = \frac{E_{dc}}{2\pi} \int_0^{\pi} I_{max} \sin \Omega t \, d(\Omega t)$$

$$= \frac{E_{dc} I_{max}}{\pi} = \frac{32.3}{\pi} = 10.3 \text{ watt}$$

There are two sub-systems and each has two transistor circuits. The loss for the system is:

Transistor Circuit Loss = 10.3 x 4 = 41.2 watts

or 20.6 watts/bearing.

This transistor circuit loss is to replace the copper loss.

7. Bearing Film Loss

The loss in the bearing film is predominantly frictional loss due to shear. The shear stress is equal to the product of viscosity and velocity gradient,

$\mu \frac{\omega(D/2)}{C}$; the effect of eccentricity has been neglected.

To obtain power loss, we should multiply the shear stress by an area (πDL), and a velocity $\omega D/2$. Thus,

$$\text{Bearing film loss} = \mu \frac{\omega D/2}{C} (\pi DL) \frac{\omega D}{2}$$

With

$\mu = 2.7 \times 10^{-9}$ lb-sec/in^2

$\omega = 1255$ rad/sec

$D = L = 3.5$ inches

$C = \begin{cases} 0.001 \text{ inch for unidirectional device} \\ 0.002 \text{ inch for active device} \end{cases}$

we calculate

$$\text{Bearing film loss} = \begin{cases} 56.5 \text{ watts/bearing for unidirectional device} \\ 28.3 \text{ watts/bearing for active device} \end{cases}$$

8. Total Power Loss

The total power loss is the sum of eddy-current loss, hysteresis loss, copper loss and bearing film loss. Thus,

Total Power Loss = 1.1 + 0.036 + 2.3 + 2 x 56.5

= 116.4 watts for unidirectional device

Total Power Loss = 1.6 + 0.005 + 140 + 2 x 28.3

= 198.2 watts for active device with external resistance

Total Power Loss = 1.6 + 0.005 + 41.2 + 2 x 28.3

= 99.4 watts for active device with transistor circuits.

The above power losses are to be compared with the loss in the tilting pad gas bearings currently in use; it was reported to be 180 watts for the two bearings.

9. Weight Penalties

a. Unidirectional Device

The laminated disk has a thickness of 4 inches, and outside and inside diameters of 6 in. and 4 in. respectively (See Section IV-4).

Volume of Laminated Disk = $4 \times \frac{\pi}{4} (6^2 - 4^2) = 62.8$ in^3

Weight of Laminated Disk = Density x Volume = 0.317 x 62.8

= 19.9 lb. (Supermalloy)

The Density of Supermalloy is 0.317 lb/in^3

Volume of Magnet Core = $(w \times d)(\ell_w + d + \ell'_w + d)2$

= $(4 \times 0.92)(1.25 + 0.92 + 1 + 0.92)2$

= 30.3 in^2

Weight of Magnet Core = Density x Volume = 0.317 x 30.3 = 9.6 lb. (Supermalloy)

Volume of Coil Winding = $(\ell_w \times \ell'_w)(d + \ell'_w + w + \ell'_w)2$

= $(1.25 \times 1)(0.92 + 1 + 4 + 1)2 = 17.3$ in^3

From Section IV-1, the cross sectional areas of the copper and the insulation in the winding are respectively 0.48 in^2 and 0.75 in^2. Therefore, the volumetric percentage of copper in the winding is 0.48/(0.48 + 0.75) = 39%, and the remaining 61% is insulation. The density of copper is 0.324 lb/in^3. Assume the density of insulation to be 0.065 lb/in^3 (20% of copper density). Then, the density of the coil winding is (0.324 x 0.39 + 0.065 x 0.61) = 0.166 lb/in^3.

Weight of Coil Winding = Density x Volume = 0.166 x 17.3 = 2.87 lb.

Since only a-c power is available from the turboalternator and d-c power is needed for the electromagnet, a rectifier is required whose weight is estimated at 0.5 lb.

Total Weight Penalty = 19.9 + 9.6 + 2.87 + 0.5 = 32.9 lb.

b. Active Device

The laminated disk has a thickness of 1 inch, and outside and inside diameters of 6 in. and 4 in. respectively (See Section IV-4).

Volume of Laminated Disk = $1 \times \frac{\pi}{4} (6^2 - 4^2)$
= 15.7 in^3

Weight of Laminated Disk = Density x Volume = 0.317 x 15.7 = 4.98 lb. (Supermalloy)

Volume of One Magnet Core = (w x d) (ℓ_w + d + ℓ'_w + d)2
= (1.1 x 1.1) (1 + 1.1 + 0.62 + 1.1)2
= 9.2 in^3

Weight of One Magnet Core = Density x Volume = 0.317 x 9.2
= 2.92 lb. (Supermalloy)

Volume of One Coil Winding = (ℓ_w x ℓ'_w) (d x ℓ'_w + w + ℓ'_w)2
= (1 x 0.62) (1.1 + 0.62 + 1.1 + 0.62)2
= 4.26 in^3

The density of coil winding is as shown in Section IV-9-a, 0.166 lb/in^3.

Weight of One Coil Winding = Density x Volume = 0.166 x 4.26 = 0.708 lb.

Total Weight of Disk, and Four Sets of Magnet and Coil Winding

= 4.98 + 4 (2.92 + 0.708) = 19.5 lb.

Allow three pounds for the amplifier-transformer unit and 0.5 lb. for the probe, differentiator and signal splitter (See Fig. 8); and there are two subsystems in the active device.

Total Weight Penalty = 19.5 + 2 (3 + 0.5) = 26.5 lbs.

SUMMARY

The major results of this feasibility study are summarized as follows:

1. Two devices appear to be feasible to improve the stability of rotor-bearing systems.

   A. Unidirectional Device--producing a unidirectional magnetic force to load the bearing.

   B. Active Device--producing a controlled electromagnetic force always opposing the motion of the shaft.

2. Plain journal bearings operating in a zero-g environment can be made stable by using either the unidirectional device or the active device; the stability margin achieved by the unidirectional device is at best equal to that of a gravity-loaded bearing if Λ is large or moderately large ($\Lambda \gtrsim 0.3$ roughly).

3. The active device is very effective in suppressing whirl instabilities. A nominal magnetic damping produced by the active device can increase the critical mass several-fold. Preliminary calculation shows that for $\Lambda = 1.0$, the critical mass is increased 100 times with a $V_{mxx} = V_{myy} = 0.1$ which can be easily achieved. The effect becomes even more profound for smaller Λ, but less for larger Λ.

4. The magnetic damping produced by the active device is not linear with the rotor displacement. A quasi-linear approach is used in the critical mass calculation.

5. There are two possible ways to make the magnetic damping linear. One is to use square root function generators, and the other is to apply a d-c current bias. Both methods have their shortcomings as stated in the text. We do not recommend to use either of the two until it is proven that the linear magnetic damping is superior to the non-linear one.

6. A 9 kw turboalternator supported by two tilting pad gas bearings was used as a reference to assess the power loss and weight penalties associated with the use of either device. They are listed in the following.

Plain Journal Bearings with Unidirectional Device

Power Loss = 116.4 watts
Weight Penalty = 32.9 lbs.

Plain Journal Bearings with Active Device

Power Loss = 99.4 watts
Weight Penalty = 26.5 lbs.

Comparing with the rotor weight of 56 lbs., the weight penalty of using either device is appreciable. The above power losses compare favorably with the existing bearing system as the frictional loss in the two gas bearings of tilting-pad design was reported to be 180 watts.

RECOMMENDATIONS

It is recommended to design and fabricate a rotor-bearing unit employing plain journal gas bearings and the active electromagnetic device. The rotor-bearing system should be designed to be in a dynamically unstable condition without the aid of the active device. By switching the active device on and off, one would be able to demonstrate its effectiveness in suppressing the whirl instability of the rotor.

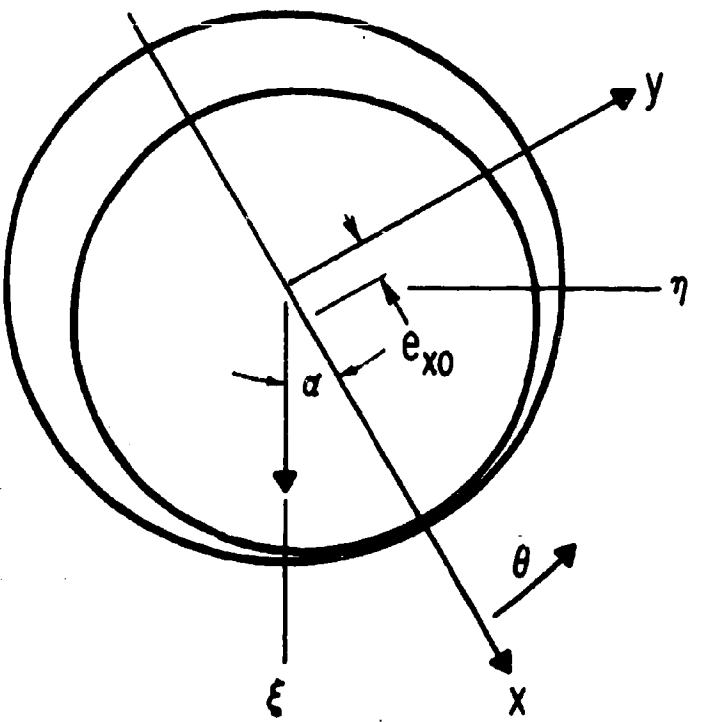

Fig. 1 Coordinate System of a Cylindrical Journal Bearing

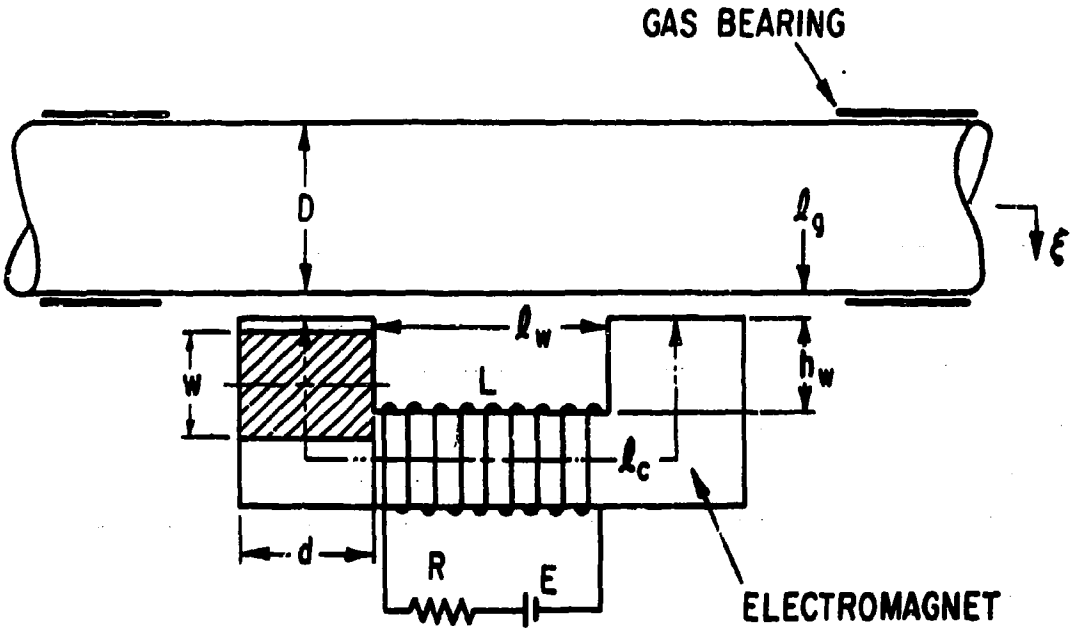

Fig. 2 Schematic Diagram of a Unidirectional Device

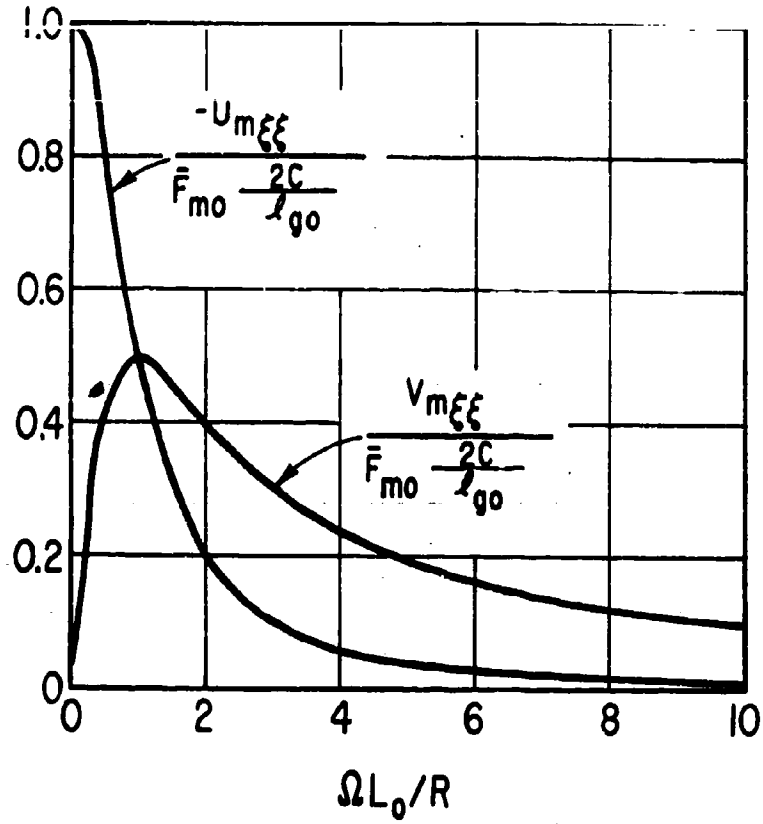

Fig. 3 Magnetic Stiffness and Damping versus $\Omega L_0/R$

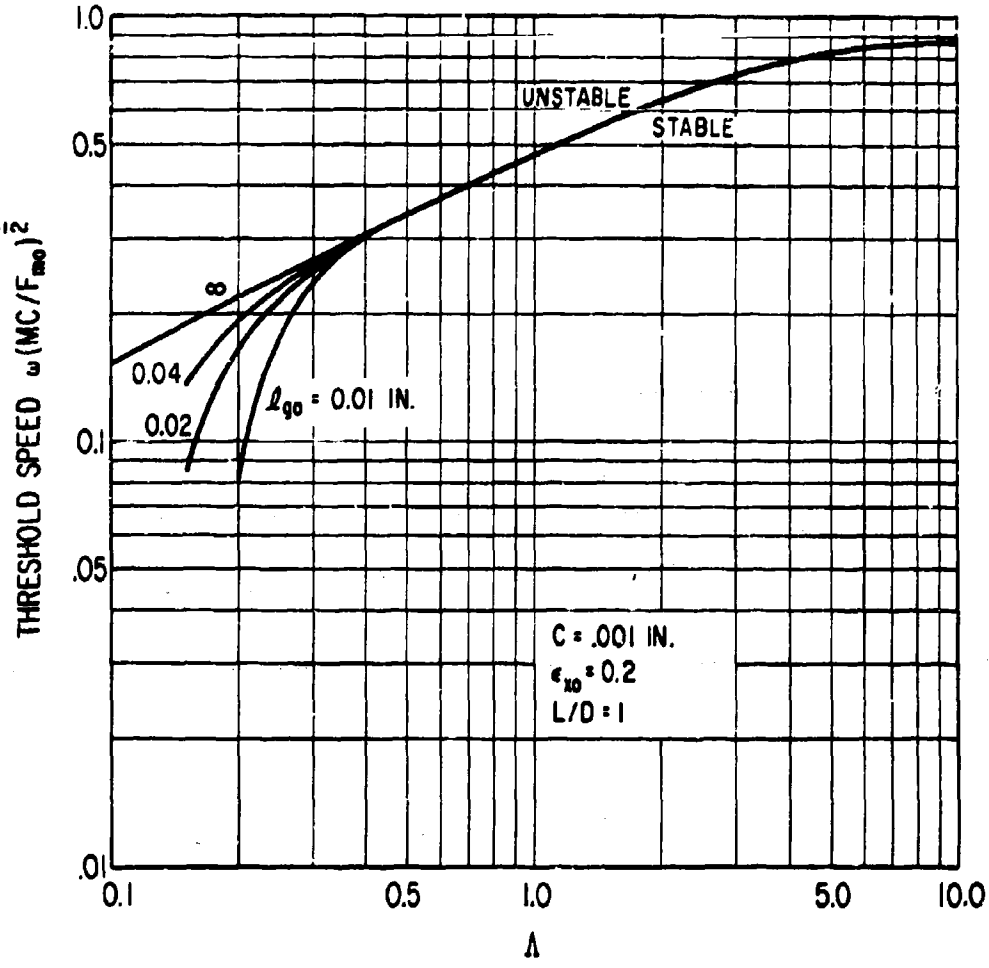

Fig. 4 Threshold Speed Against Λ at $\epsilon_{xo} = 0.2$

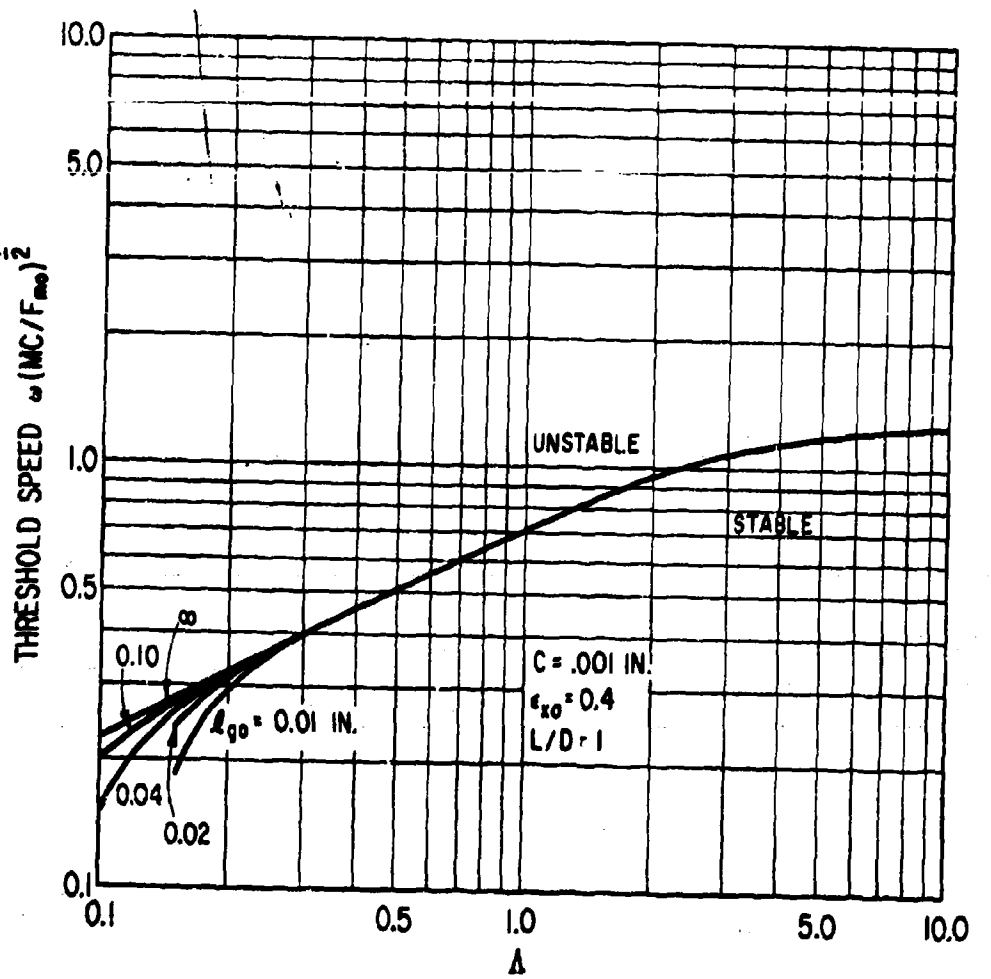

Fig. 5 Threshold Speed Against Λ at $\epsilon_{xo} = 0.4$

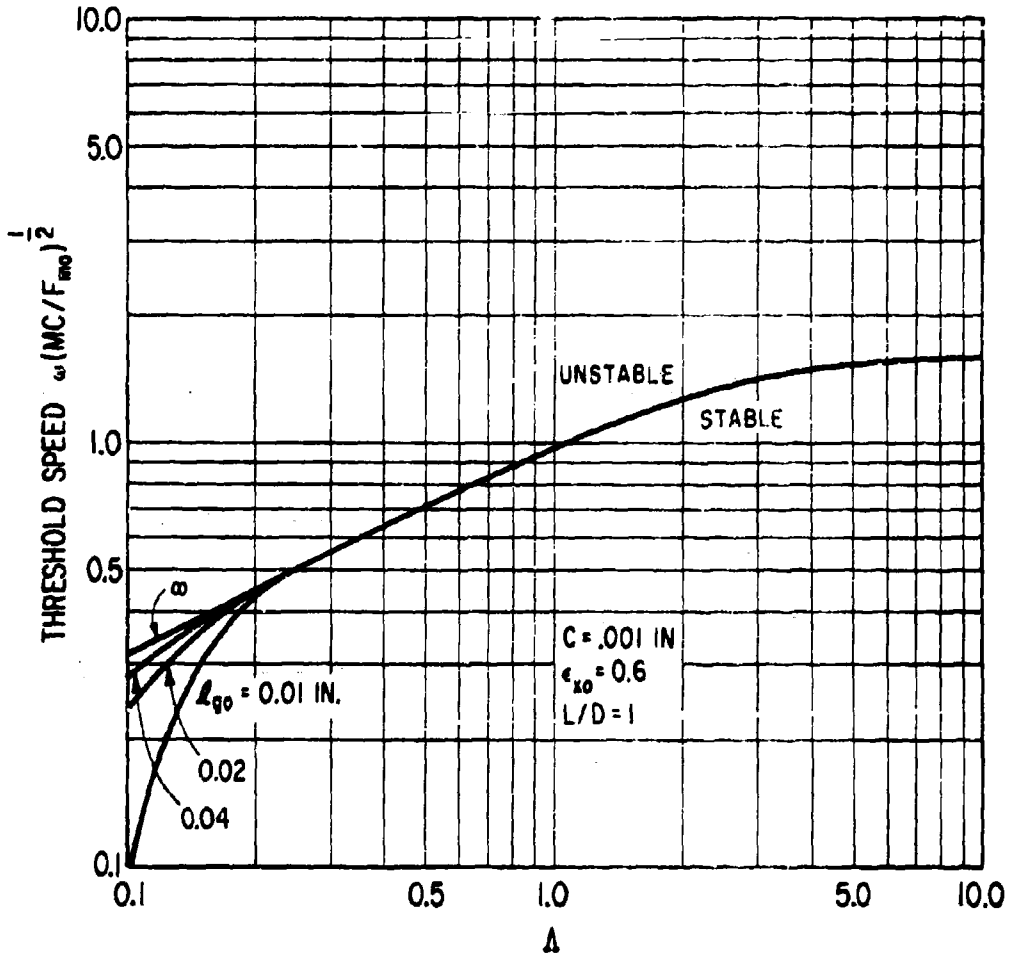

Fig. 6 Threshold Speed Against Λ at $\epsilon_{xo} = 0.6$

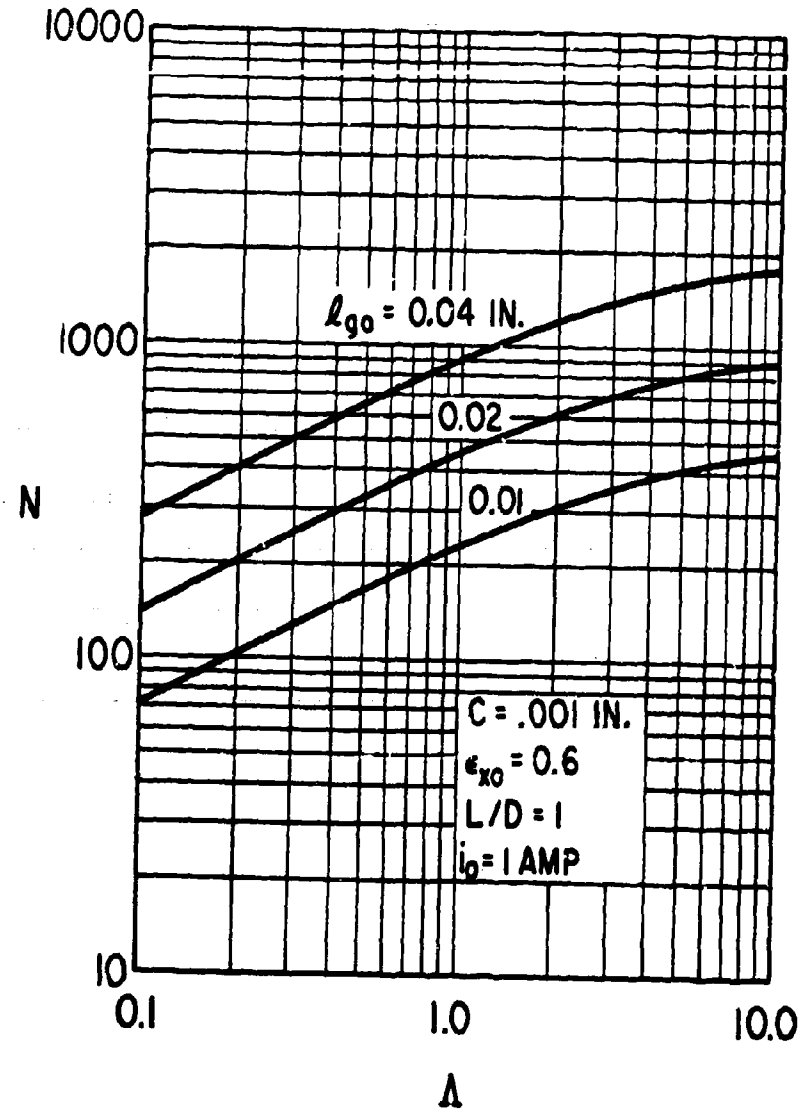

Fig. 7 Number of Turns Against Λ

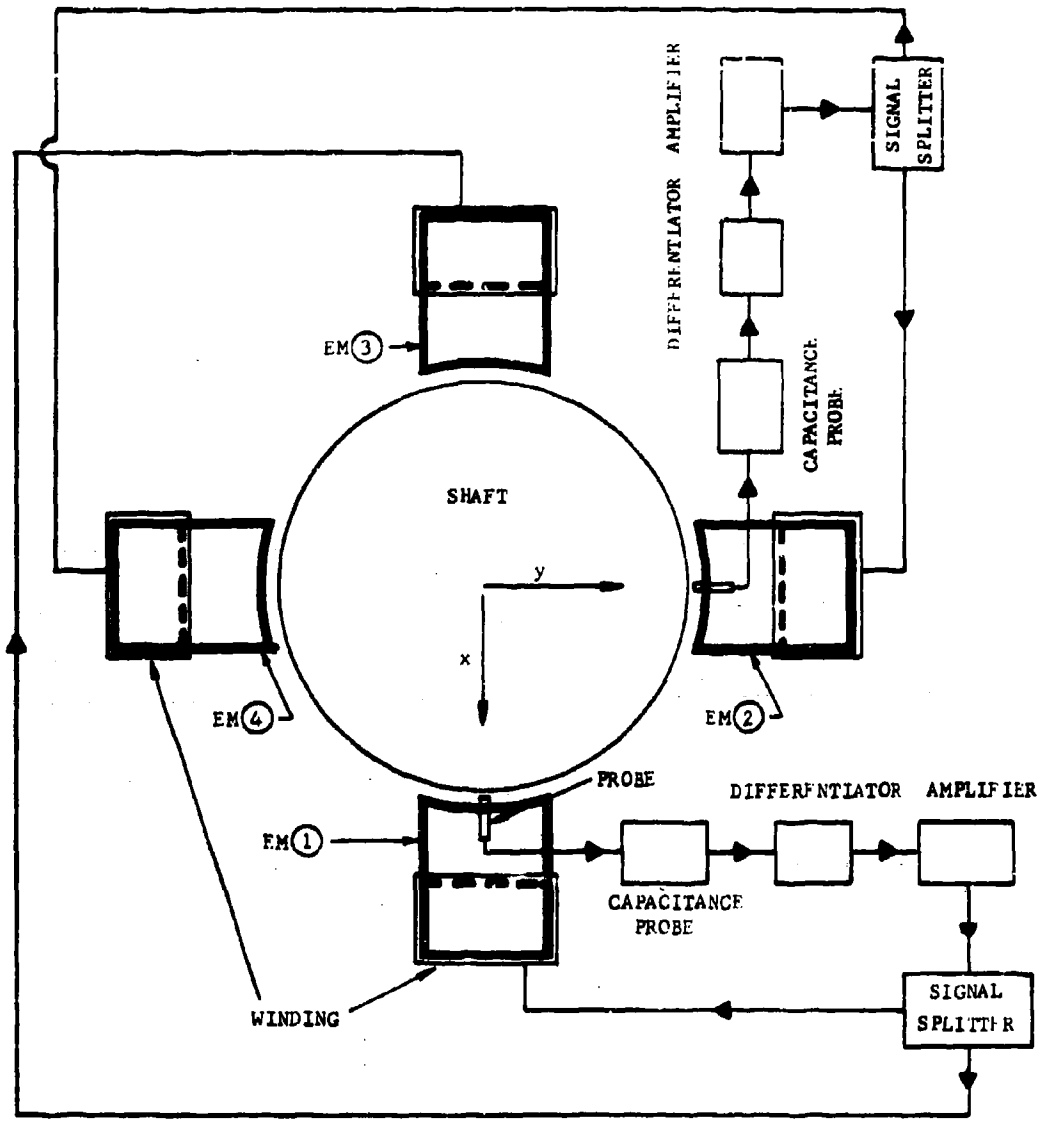

Fig. 8 Schematic Diagram of an Active Device

MTI-8586

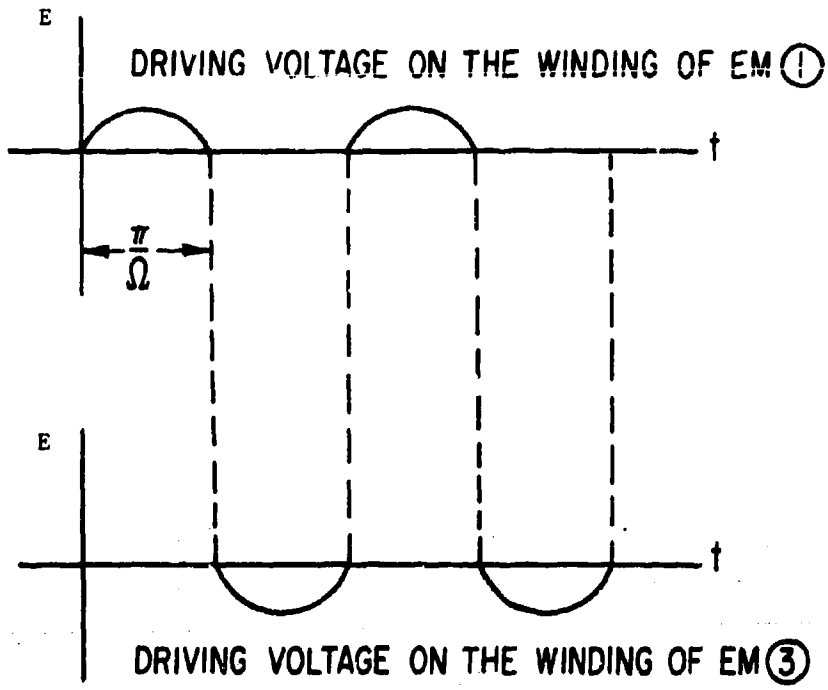

Fig. 9 Illustrations of the Driving Voltage as a Function of Time

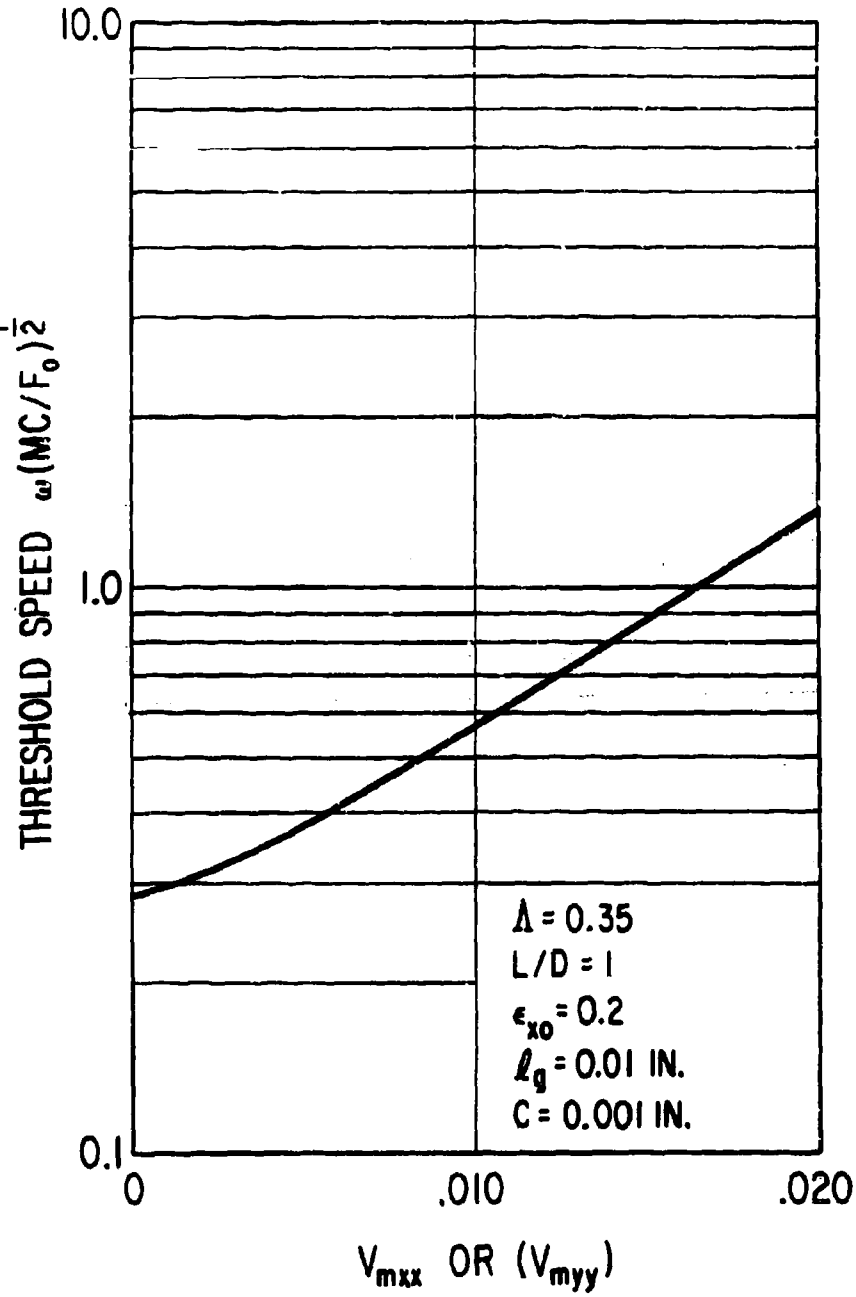

Fig. 10 Threshold Speed versus Dynamic Magnetic Damping at $\Lambda = 0.35$

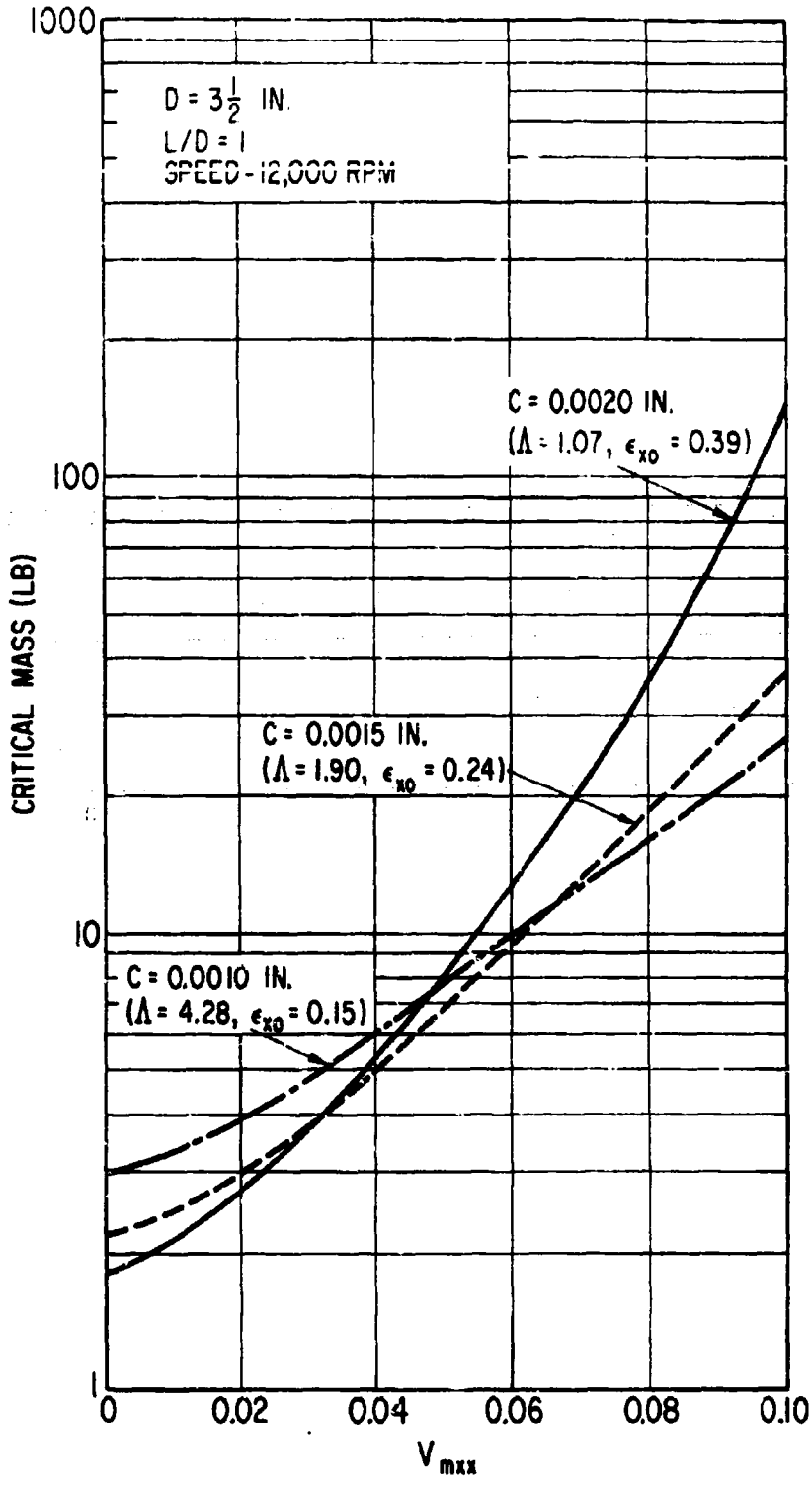

Fig. 11 Critical Mass versus Dynamic Magnetic Damping under Gravitational Loading

MII-8582

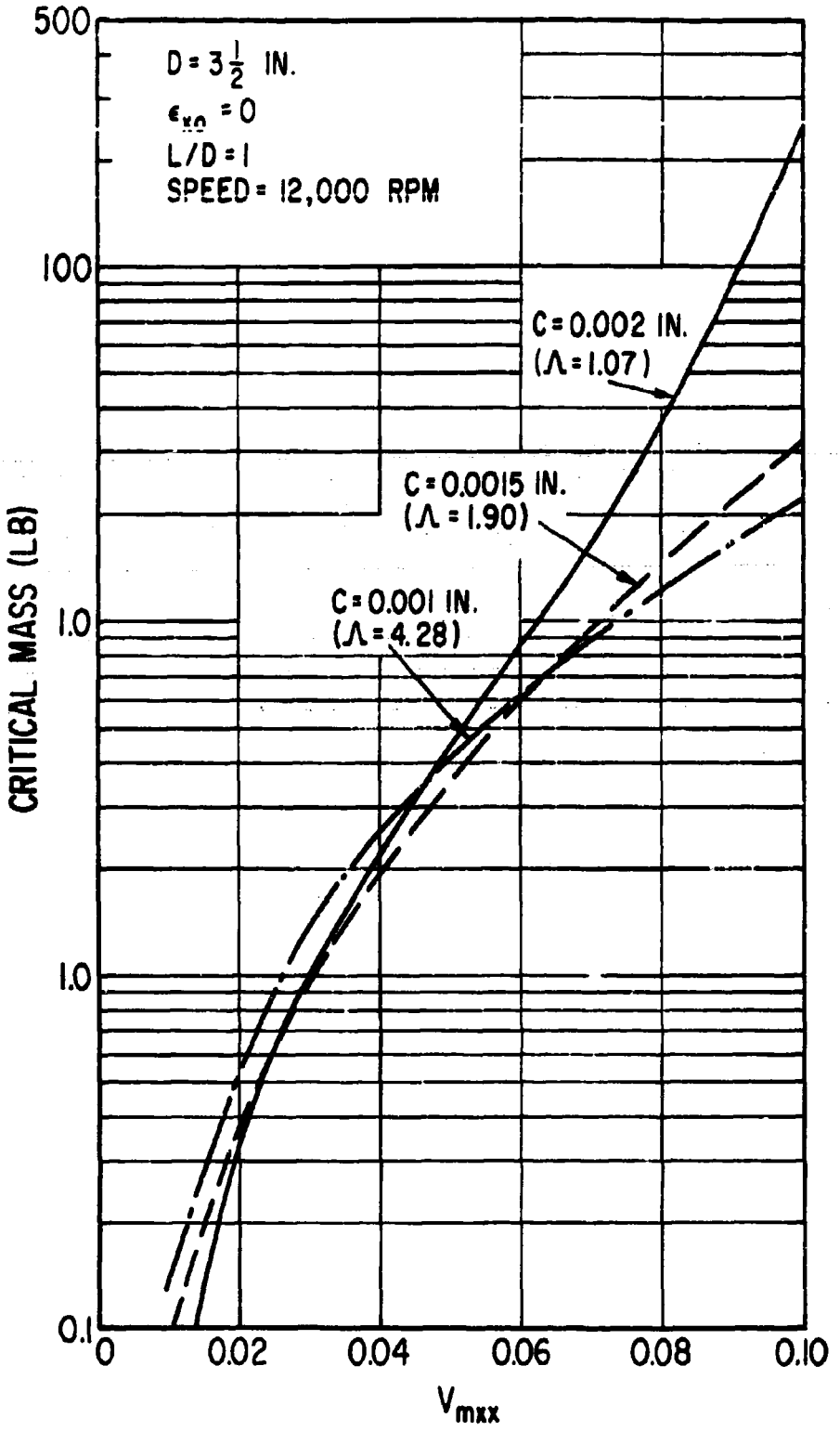

Fig. 12 Critical Mass versus Dynamic Magnetic Damping at Unloaded Condition

MTI-8585

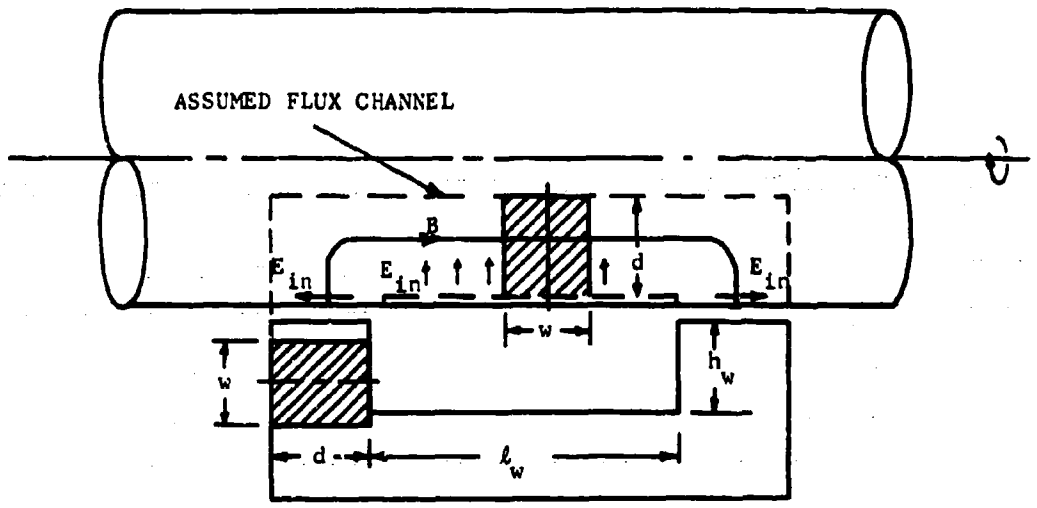

Fig. 13 Model of Magnetic Flux Channel for Eddy-Current Loss Analysis

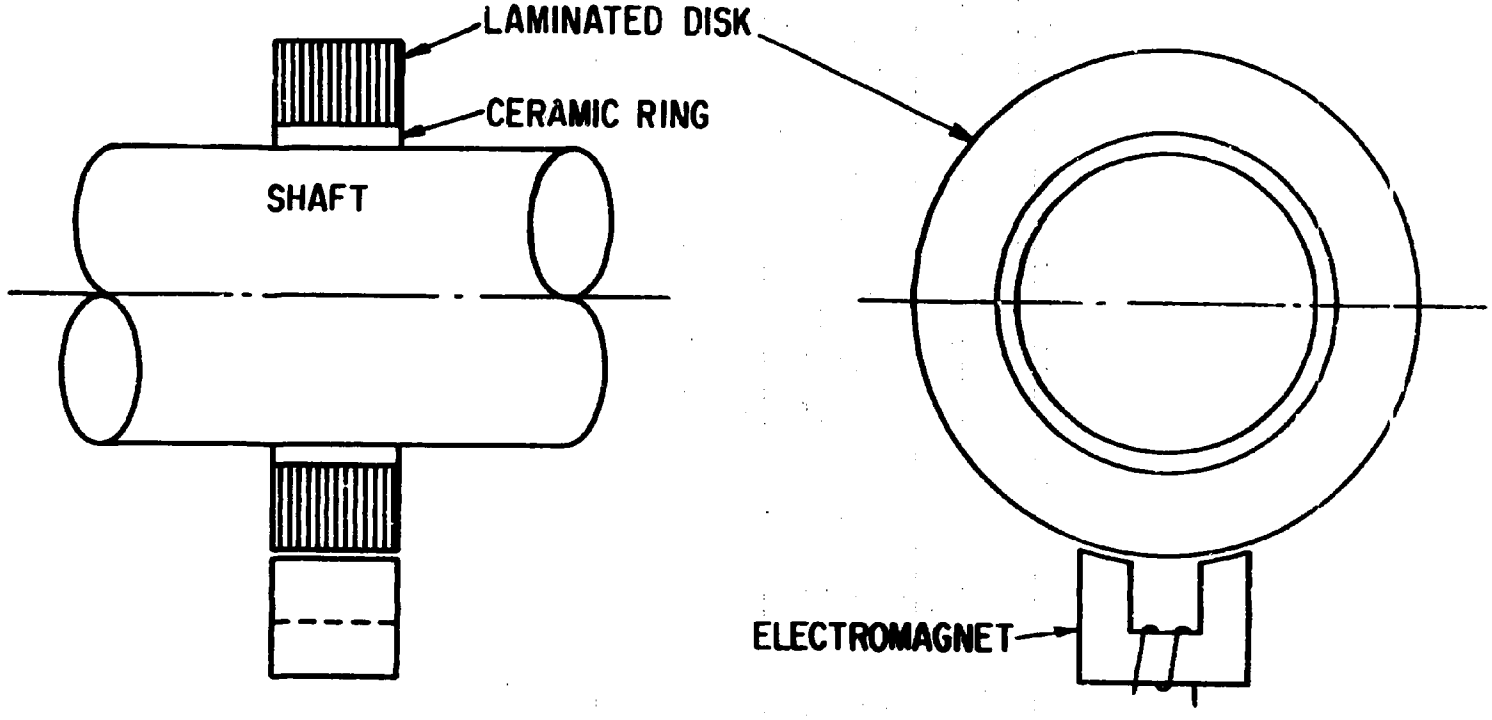

Fig. 14 Unidirectional Device with a Laminated Disk

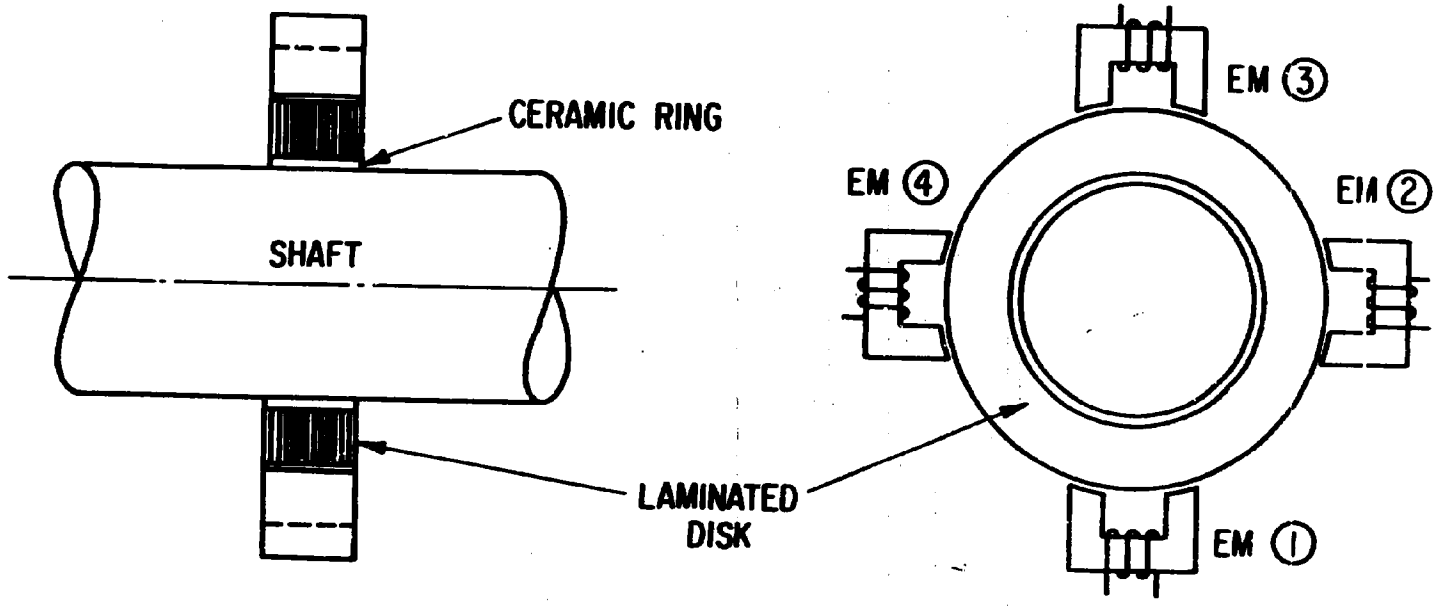

Fig. 15 Active Device with a Laminated Disk

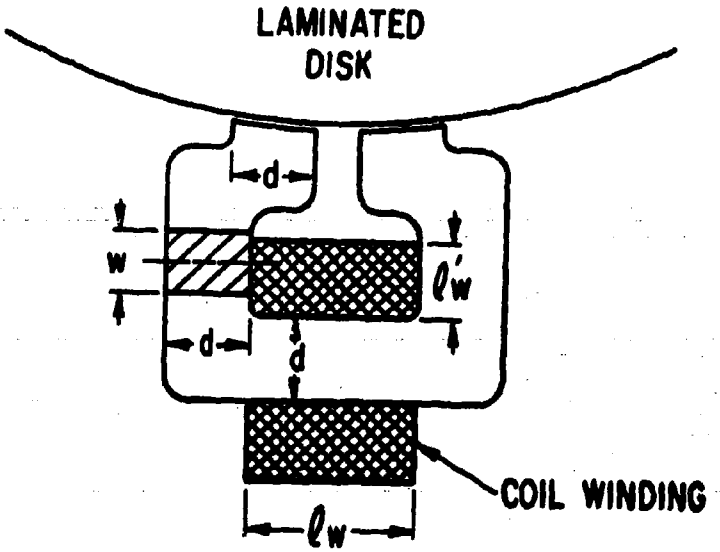

Fig. 16 Configuration of Electromagnet in Association with a Laminated Disk

APPENDIX I: Definition of Quantities Associated with the Bearing Mechanical Impedance

The following definitions were given in [5]. They are listed below for easy reference

$$E_1 = \frac{2}{\varepsilon_{xo}^2\sqrt{1-\varepsilon_{xo}^2}}\left[1 - \sqrt{1-\varepsilon_{xo}^2}\right]$$

$$E_2 = \frac{2}{\varepsilon_{xo}^2}\left[1 - \sqrt{1-\varepsilon_{xo}^2}\right]$$

$$E_3 = \frac{2}{\varepsilon_{xo}^3(1-\varepsilon_{xo}^2)^{3/2}}\left\{2\left[(1-\varepsilon_{xo}^2)^{3/2} - 1\right] + 3\varepsilon_{xo}^2\right\}$$

$$E_4 = \frac{2}{\varepsilon_{xo}^3(1-\varepsilon_{xo}^2)^{3/2}}\left\{\varepsilon_{xo}^2(\varepsilon_{xo}^2 - 3) + 2\left[1 - (1-\varepsilon_{xo}^2)^{3/2}\right]\right\}$$

$$F + iG = \frac{1}{2}\left(\frac{D}{L}\right)\int_{-L/D}^{L/D}(u + iv)d\zeta$$

$$\begin{Bmatrix} F_{(\pm)} \\ G_{(\pm)} \end{Bmatrix} = \begin{Bmatrix} F(\Lambda_{(\pm)},\ L/D) \\ G(\Lambda_{(\pm)},\ L/D) \end{Bmatrix}$$

$$\Lambda_{(\pm)} = \Lambda(1 \pm 2f)$$

u and v are functions of Λ, L/D and ζ; they are given in [7] and Eq. (68) of [5]

$$Z_{xx} = -\frac{1}{2}\left[\varepsilon_{xo}E_3F + E_1(K_{/} + if\omega C_{/})\right]$$

$$Z_{xy} = -\frac{1}{2}\left[-\varepsilon_{xo}E_4G + E_1(K_{\perp} + if\omega C_{\perp})\right]$$

$$Z_{yx} = +\frac{1}{2}\left[-\epsilon_{xo}E_4G - E_2(K_\perp + if\omega C_\perp)\right]$$

$$Z_{yy} = +\frac{i}{2}\left[\epsilon_{xo}E_4F + E_2(K_{||} + if\omega C_{||})\right]$$

where

$$K_{||} = \frac{1}{2}\left[F_{(-)} + F_{(+)}\right]$$

$$f\omega C_{||} = -\frac{i}{2}\left[G_{(-)} - G_{(+)}\right]$$

$$K_\perp = \frac{1}{2}\left[G_{(-)} + G_{(+)}\right]$$

$$f\omega C_\perp = \frac{1}{2}\left[F_{(-)} - F_{(+)}\right]$$

In Appendix IV, where harmonics of the whirl frequency are considered, the following nomenclature is used:

$$Z_{xxn} = U_{xxn} + iV_{xxn} \qquad \text{etc.}$$

n being the harmonic number, n = 1, 2, 3, In particular, for $\epsilon_{xo} = 0$ and n = 1,

$$U_{xx1} = U_{yy1} = U_{||1} = K_{||}$$

$$V_{xx1} = V_{yy1} = V_{||1} = f\omega C_{||}$$

$$U_{xy1} = U_{yx1} = U_{\perp 1} = K_\perp$$

$$V_{xy} = V_{yx1} = V_{\perp 1} = f\omega C_\perp$$

APPENDIX II: Differentiator and Signal Splitter

In an active device, differentiators and signal splitters are required as indicated in the text. Their operating principles and circuit diagrams will be illustrated here.

A standard differentiator circuit shown below can be assembled to perform the differentiation operation upon the input voltage which in this particular application is the output of the displacement probe. In the sketch, A is an

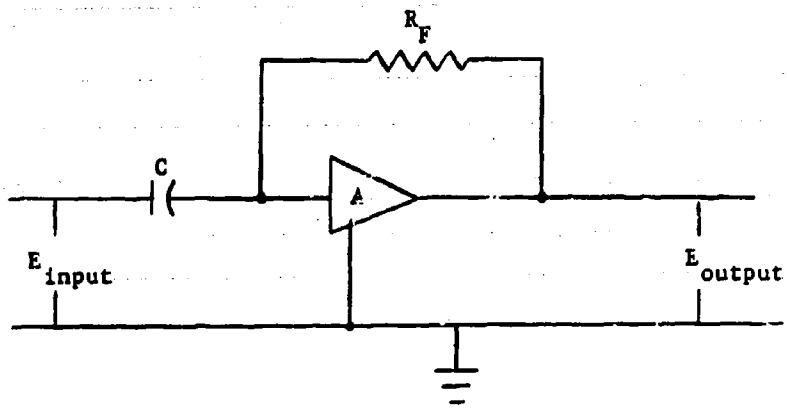

Differentiator Circuit

operational amplifier, C a capacitor and R_F a resistor. The resistor and the operational amplifier form a feedback network to regulate the gain. The capacitor and this feedback network would then perform the differentiation operation. A more detailed explanation on the differentiator circuit can be found in [8].

A signal splitter consists of two diodes D_1 and D_2 as shown in the sketch.

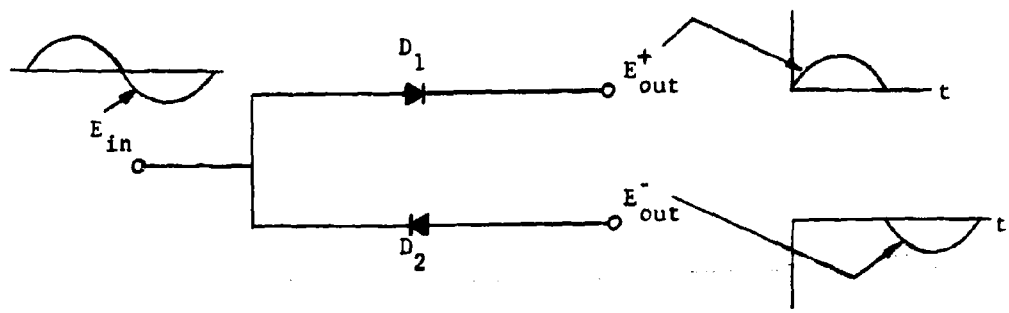

Signal Splitter

The two diodes are connected so that a positive-going signal will be routed to E^+_{out} and a negative-going signal will be routed to E^-_{out}. The two output terminals are to be connected to the two coil windings of, say, EM (1) and EM (3) of Fig. 8.

APPENDIX III: Computer Program - PN 424 - Influences of Magnetic Forces (Unidirectional or by an Active Device) on Stability of Plain Journal Bearings

INPUT

Card 1 (80H) — Title card

Card 2 (8E10.3) — This card contains the following five values:

- ℓ_g = magnetic air gap [in]
- C = radial bearing clearance [in]
- μ = viscosity [lb-sec/in^2]
- p_a = ambient pressure [lb/in^2]
- D = diameter of shaft [in]

Card 3 (8E10.3) — This card contains the following three dimensionless quantities:

- f_a = initial value of frequency ratio f
- f_b = final value of frequency ratio f
- Δf = increment used in scanning frequency ratios from f_a to f_b

Card 4 (8E10.3) — This card contains the following three dimensionless quantities:

- Λ = compressibility number
- ϵ_{xo} = dimensionless bearing steady-state displacement
- L/D = bearing length diameter ratio

Card 5 (4I5) — This card contains the following four control integers: MORE, MD, MP, MACT

- MORE = 1, another case to follow
  0, this is the last case
- MD = 1, print E_1, E_2, E_3, E_4
  0, print basic quantities only in the output

MP = 0, take positive sign for complex square root

-1, take negative sign for complex square root

MACT = 0, for unidirectional device

1, for active device

Card 5* (8E10.3) — If MACT = 1, two cards containing the following information are needed:

U_{mxx}, U_{mxy}, U_{myx}, U_{myy}

V_{mxx}, V_{mxy}, V_{myx}, V_{myy}

Card 5** (8E10.3) — If MACT = 0, one card containing the following four values is needed instead:

A_g = area of magnetic air gap [in^2]

A_k = area of conductor [cir. mil]

ℓ_k = length of conductor [in]

i = current [amp]

Card 6 (I1,E14.7) — Change cards containing one integer code and one real number. The real number replaces the current value of an input quantity designated by the following code:

Code 1. ℓ_g

Code 2. C

Code 3. Λ

Code 4. ϵ_{xo}

Card 7 — Blank card

Cards 6 and 7 may be repeated as many times as desired.

Card 8 — An additional blank card to terminate

The entire above sequence may be repeated as many times as desired with MORE = 1.

OUTPUT

Each output page is for a particular value of f, the frequency ratio. It will begin with $f = f_a$ and increase with increment Δf until either a critical frequency ratio is found or the final value $f = f_b$ is reached. The following is an illustration of a typical output page:

Line 1. Frequency ratio

Line 2.
FP = F(+)
FM = F(-)
CAP-F = F
See Appendix I

Line 3.
GP = G(+)
GM = G(-)
G = C
See Appendix I

Line 4
K(PARL) = $K_{//}$ = Bearing stiffness in line with line of centers of bearing and journal

F*OMEGA*C(PARL) = $f\omega C_{//}$ = Parallel damping in line with line of centers of bearing and journal

K(PERP) = $K_{\perp}$ = Bearing stiffness normal to line of centers of bearing and journal

F*OMEGA*C(PERP) = $f\omega C_{\perp}$ = Bearing damping normal to line of centers of bearing and journal

Line 5.
W-SUB-XO = W_{xo} [dimensionless]

W-SUB-YO = W_{yo} [dimensionless]

ALPHA = α = attitude angle

F-BAR = $\bar{F}_m = [(W_{xo})^2 + (W_{yo})^2]^{1/2}$, [dimensionless]

Line 6. F-SUB-M = $F_m = \bar{F}_m \pi DLp_a$, [lb]

K-SUB-M = $\bar{k}_m$ = $-2 \frac{c}{\ell_g} \bar{F}_m$ [dimensionless]

K-SUB-MX = $\bar{k}_{mx}$ = $\bar{k}_m \cos \alpha$ [dimensionless]

K-SUB-MY = k_{my} = $\bar{k}_m \sin \alpha$ [dimensionless]

Lines 7 & 8. Systems dynamic stiffness and damping including those contributed by bearing film forces and magnetic forces.

Line 9. A = A_1

B = B_1

ZR = Z_r

ZI = Z_i

Line 10. W(F) = left hand side of (11)

Line 11. This additional line will show only on the last output page, if a critical frequency ratio is found.

M = m_c = dimensionless critical mass

CAP-M = M = critical mass [lb]

T.S. = threshold speed [dimensionless]

A Fortran listing of program PN 424 is provided in the next few pages. Typical listings of input and output are also given.

```
// FOR TOM5
*IOCS(CARD,1443 PRINTER)
*NONPROCESS PROGRAM
*ONE WORD INTEGERS
*LIST ALL
*PUNCH
C
C      INFLUENCE OF MAGNETIC FORCES
C      (UNIDIRECTIONAL OR BY AN ACTIVE DEVICE)
C      ON STABILITY OF PLAIN JOURNAL BEARING
C      B.BRYNOLFSON FOR T.CHIANG          2/23/68
C
C
C      INPUT FOR TOM5
C
C      1.   (80H)          TITLE CARD
C      2.   (8E10.3)       SMALL L,C,MU,P-SUB-A,D
C      3.   (8E10.3)       F-SUB-A,F-SUB-B,DELTA-F
C      4.   (8E10.3)       LAMBDA,EPSILON-SUB-X0,CAP-L/D
C      5.   (4I5)          MORE,MD,MP,MACT
C                          MORE=1 ANOTHER CASE TO FOLLOW
C                          MORE=0  THIS IS LAST CASE
C                          MD=1 PRINT E1,E2,E3,E4
C                          MD=0 ONLY BASIC PRINT
C                          MP=0     + SIGN FOR COMPLEX SQUARE ROOT
C                          MP=-1    - SIGN FOR COMPLEX SQUARE ROOT
C                          MACT=0 UNIDIRECTIONAL MAGNETIC FORCE
C                          MACT=1 MAGNETIC FORCE FROM ACTIVE DEVICE
C      5+   (8E10.3)       IF MACT=1,  TWO(2) CARDS AS FOLLOWS
C                          AUXX, AUXY, AUYX, AUYY
C                          AVXX, AVXY, AVYX, AVYY
C      5++  (8E10.3)       IF MACT=0,  ONE CARD AS FOLLOWS
C                          AG,AK,LK,I
C      6.   (I1,E14.7)     CHANGE CARDS
C      7.                  BLANK CARD
C      ITEMS 6. AND 7. MAY BE REPEATED AS MANY TIMES AS DESIRED
C      8.                  AN ADDITIONAL BLANK CARD TO TERMINATE
C
C      THE ENTIRE ABOVE SEQUENCE MAY BE REPEATED AS MANY TIMES AS DESIRED
C      WITH MORE=1
C
C
C      CHANGE CARDS CONTAIN ONE INTEGER CODE AND ONE REAL NUMBER.
C      THE REAL NUMBER REPLACES THE CURRENT VALUE OF AN INPUT QUANTITY
C      DESIGNATED BY THE INTEGER CODE.
C      THE CODES AND THEIR CORRESPONDING QUANTITIES ARE
C      1    SMALL L
C      2     C
C      3     LAMBDA
C      4     EPSILON-SUB-X0
C
C
      DIMENSION W(30),FF(30)
C
      DATA NR,NW/2,3/
      DATA RD2DG, PI/57.29578,3.1415926535/
C
      CALL TEST
      CALL DUMPP
    1 READ (NR,2000)
```

```
      READ (NR,2010) EL,C,ZMU,PSUBA,D
      READ (NR,2010) FA,FB,DELF
      READ (NR,2010) ZLAM,EPS,ELOVD
      READ (NR,2020) MORE,MD,MP,MACT
      IF (MACT) 9,9,5
    5 READ (NR,2010) AUXX,AUXY,AUYX,AUYY
      READ (NR,2010) AVXX,AVXY,AVYX,AVYY
      GO TO 10
C
    9 READ (NR,2010) AG,AK,ELK,QI
   10 WRITE(NW,3000)
      WRITE(NW,2000)
      WRITE(NW,3001)
      WRITE(NW,3010) EL,C,ZMU,PSUBA,D
      WRITE(NW,3002)
      WRITE(NW,3010) FA,FB,DELF
      WRITE(NW,3003)
      WRITE(NW,3010) ZLAM,EPS,ELOVD
      WRITE(NW,3004)
      WRITE(NW,3020) MORE,MD,MP,MACT
      IF (MACT) 15,15,14
   14 WRITE(NW,3022)
      WRITE(NW,3010) AUXX,AUXY,AUYX,AUYY
      WRITE(NW,3023)
      WRITE(NW,3010) AVXX,AVXY,AVYX,AVYY
      GO TO 16
   15 WRITE(NW,3025)
      WRITE(NW,3010) AG,AK,ELK,QI
C
   16 CAPL=D*ELOVD
      OMEGA=2.0*C/D
      OMEGA=ZLAM*PSUBA*OMEGA*OMEGA/(6.0*ZMU)
      WRITE(NW,3017)
      WRITE(NW,3010) OMEGA
      CALL EPFUN(EPS,E1,E2,E3,E4)
      IF (MD) 22,22,21
   21 WRITE(NW,3005)
      WRITE(NW,3010) EPS,E1,E2,E3,E4
   22 EN=0.0
      I=0
      J=1
   25 F=FA+EN*DELF
      FF(J)=F
      IF (FB-F) 150,30,30
   30 WRITE(NW,3101) F
      CALL KCEFG(F,ZLAM,ELOVD,FP,FM,CAPF,GP,GM,CAPG,ZKPLL,FCPLL,ZKPRP,
     *FCPRP)
      IF (MD) 32,32,31
C
   31 WRITE(NW,3014)
      WRITE(NW,3010)  FP,FM,CAPF
      WRITE(NW,3015)
      WRITE(NW,3010)  GP,GM,CAPG
      WRITE(NW,3016)
      WRITE(NW,3010)  ZKPLL,FCPLL,ZKPRP,FCPRP
   32 WX0=-0.5*EPS*E1*CAPF
      WY0=0.5*EPS*E2*CAPG
      ALFA=ATAN(-WY0/WX0)
      ALFDG=ALFA*RD2DG
      FMBAR=SQRT(WX0*WX0+WY0*WY0)
```

```
      WRITE(NW,3006)
      WRITE(NW,3010) WXO,WYO,ALFDG,FMBAR
C
      FM=FMBAR*PI*D*PSUBA*CAPL
      ZKM=-2.0*C*FMBAR/EL
      CSALF=COS(ALFA)
      SNALF=SIN(ALFA)
      ZKMX=ZKM*CSALF
      ZKMY=ZKM*SNALF
      CSA2=CSALF*CSALF
      CSSN=CSALF*SNALF
      SNA2=SNALF*SNALF
      WRITE(NW,3007)
      WRITE(NW,3010) FM,ZKM,ZKMX,ZKMY
C
      UXX=0.5*(EPS*E3*CAPF+E1*ZKPLL)
      UYX=-0.5*(EPS*E4*CAPG+E2*ZKPRP)
      UXY=0.5*(E1*ZKPRP-EPS*E4*CAPG)
      UYY=0.5*(EPS*E4*CAPF+E2*ZKPLL)
      IF (MACT) 33,33,34
C
C     MODIFIED 4/68 - NEW COEFFICIENTS FOR UNIDIRECTIONAL CASE
   33 B=SQRT(72.0E6*FM/AG)
      QN=0.62*B*EL/QI
      RE=0.867*QN*ELK/AK
      ELZRO=QN*B*AG*1.0E-8/QI
      ROVL=RE/ELZRO
      WRITE(NW,3026)
      WRITE(NW,3010) B,QN,RE,ELZRO
      FOMEG=F*OMEGA
      T=FOMEG*FOMEG+ROVL*ROVL
      F1= ROVL*ROVL/T
      F2=FOME    OVL/T
      WRITE(Nw,3027)
      WRITE(NW,3010) F1,F2
      T=ZKM*F1
      BUXX=T*CSA2
      BUXY=T*CSSN
      BUYX=BUXY
      BUYY=T*SNA2
      WRITE(NW,3032)
      WRITE(NW,3010) BUXX,BUXY,BUYX,BUYY
      T=-ZKM*F2
      BVXX=T*CSA2
      BVXY=T*CSSN
      BVYX=BVXY
      BVYY=T*SNA2
      WRITE(NW,3033)
      WRITE(NW,3010) BVXX,BVXY,BVYX,BVYY
      UXX=UXX+BUXX
      UXY=UXY+BUXY
      UYX=UYX+BUYX
      UYY=UYY+BUYY
      WRITE(NW,3019)
      GO TO 1035
   34 UXX=UXX+AUXX
      UXY=UXY+AUXY
      UYX=UYX+AUYX
      UYY=UYY+AUYY
      WRITE(NW,3021)
```

```
 1035 WRITE(NW,3008)
      WRITE(NW,3010) UXX,UXY,UYX,UYY
C
      VXX=0.5*E1*FCPLL
      VYX=-0.5*E2*FCPRP
      VXY=0.5*E1*FCPRP
      VYY=0.5*E2*FCPLL
      IF (MACT) 1037,1037,1036
 1036 VXX=VXX+AVXX
      VXY=VXY+AVXY
      VYX=VYX+AVYX
      VYY=VYY+AVYY
      GO TO 1038
 1037 VXX=VXX+BVXX
      VXY=VXY+BVXY
      VYX=VYX+BVYX
      VYY=VYY+BVYY
 1038 WRITE(NW,3009)
      WRITE(NW,3010) VXX,VXY,VYX,VYY
C
      A=(UXX-UYY)**2-(VXX-VYY)**2+4.0*(UXY*UYX-VXY*VYX)
      B=4.0*(UXY*VYX+UYX*VXY)+2.0*(UXX-UYY)*(VXX-VYY)
      CALL CSQRT(A,B,ZR,ZI)
      IF(MP+1)36,35,36
   35 ZR=-ZR
      ZI=-ZI
   36 CONTINUE
      WRITE(NW,3018)
      WRITE(NW,3010) A,B,ZR,ZI
      W(J)=VXX+VYY+ZI
      WRITE(NW,3102) W(J)
C
C
      IF (I) 40,40,100
   40 IF (J-1) 99,99,45
   45 IF (W(J)*W(J-1)) 50,100,99
   50 T=(W(J)-W(J-1))/(FF(J)-FF(J-1))
      TT=W(J-1)-T*FF(J-1)
      F=-TT/T
      I=1
      GO TO 30
C
   99 EN=EN+1.0
      J=J+1
      GO TO 25
C
C 100 SMLM=UXX*VYY+UYY*VXX-UXY*VYX-UYX*VXY
C     SMLM=SMLM/(F*F*(VXX+VYY))
  100 SMLM= 0.5*(UXX+UYY+ZR)/(F*F)
      T=C*OMEGA*OMEGA*8.00259067
      EM=PI*CAPL*D*PSUBA*SMLM/T
      TS=SQRT(EM*T/FM)
      WRITE(NW,3011)
      WRITE(NW,3010) SMLM,EM,TS
      CALL TEST
C
  108 CALL MORIN(EL,C,ZLAM,EPS,I)
      IF (I) 10,10,110
  110 IF (MORE) 111,111,1
  111 CALL EXIT
```

```
C
  150 WRITE(NW,3012) FA,FB
      WRITE(NW,3013)
      J=J-1
      DO 155 I=1,J
      WRITE(NW,3030) FF(I),W(I)
  155 CONTINUE
      GO TO 100
C
C     FORMATS
 2000 FORMAT(80H
     *                              )
 2010 FORMAT(8E10.3)
 2020 FORMAT(4I5)
C
 3000 FORMAT(/1H1,26X,'INFLUENCE OF MAGNETIC FORCES',/21X,'(UNIDIRECTION
     *AL OR BY AN ACTIVE DEVICE)',/22X,'ON STABILITY OF PLAIN JOURNAL BE
     *ARING'/)
 3010 FORMAT(1X,8(3XE12.5))
 3020 FORMAT(2X,4(2XI5,2XI5,1X))
 3030 FORMAT(1X,3XE12.5,3XE12.5)
 3001 FORMAT(1HO,10X1HL,14X,1HC,13X,2HMU,11X,7HP-SUB-A,11X,1HD)
 3002 FORMAT(1HO,7X,7HF-SUB-A,8X,7HF-SUB-B,8X,7HDELTA-F)
 3003 FORMAT(1HO,8X,6HLAMBDA,8X,7HEPSILON,8X,7HCAP-L/D)
 3004 FORMAT(1HO,5X,4HMORE,3X,5HMDIAG,4X,2HMP,4X,4HMACT)
 3005 FORMAT(1HO,7X,
     *           7HEPSILON,10X,2HE1,13X,2HE2,13X,2HE3,13X,2HE4)
 3006 FORMAT(1HO,6X,8HW-SUB-X0,7X,8HW-SUB-Y0,9X,5HALPHA,10X,5HF-BAR)
 3007 FORMAT(1HO,7X,
     *           7HF-SUB-M,8X,7HK-SUB-M,7X,8HK-SUB-MX,7X,8HK-SUB-MY)
 3008 FORMAT(1HO,8X,4HU-XX,11X,4HU-XY,11X,4HU-YX,11X,4HU-YY)
 3009 FORMAT(1HO,8X,4HV-XX,11X,4HV-XY,11X,4HV-YX,11X,4HV-YY)
 3011 FORMAT(1HO,9X,1HM,12X,5HCAP-M,10X,4HT,S,)
 3012 FORMAT(6HO**** ,'W(F)=0 HAS NO ROOT ON THE CLOSED F-INTERVAL (',
     *E12.5,1H,,E12.5,1H))
 3013 FORMAT(1HO,9X,1HF,12X,4HW(F))
 3014 FORMAT(1HO,8X,2HFP, 13X,2HFM,12X,5HCAP-F)
 3015 FORMAT(1HO,8X,2HGP, 13X,2HGM,14X,1HG)
 3016 FORMAT(1HO,6X,7HK(PARL),4X,15HF*OMEGA*C(PARL),4X,7HK(PERP),4X,
     *15HF*OMEGA*C(PERP))
 3017 FORMAT(1HO,8X,5HOMEGA)
 3018 FORMAT(1HO,8X,1HA,14X,1HB,14X,2HZR,13X,2HZI)
 3019 FORMAT(1HO,'FORCE COEFFICIENTS WITH UNIDIRECTIONAL MAGNETIC FORCE'
     *)
 3021 FORMAT(1HO,'FORCE COEFFICIENTS WITH MAGNETIC FORCES GENERATED BY A
     *N ACTIVE DEVICE')
 3022 FORMAT(1HO,8X,5HAU-XX,10X,5HAU-XY,10X,5HAU-YX,10X,5HAU-YY)
 3023 FORMAT(1HO,8X,5HAV-XX,10X,5HAV-XY,10X,5HAV-YX,10X,5HAV-YY)
 3025 FORMAT(1HO,8X,2HAG,13X,2HAK,13X,2HLK,14X,1HI)
 3026 FORMAT(1HO,9X,1HB,14X,1HN,13X,2HRE,13X,2HLO)
 3027 FORMAT(1HO,8X,2HF1,13X,2HF2)
 3032 FORMAT(1HO,8X,5HBU-XX,10X,5HBU-XY,10X,5HBU-YX,10X,5HBU-YY)
 3033 FORMAT(1HO,8X,5HBV-XX,10X,5HBV-XY,10X,5HBV-YX,10X,5HBV-YY)
C
 3101 FORMAT(/1H1,15X,   3HF =,E12.5/)
 3102 FORMAT(1HO,12X,6HW(F) =,E12.5/)
C
      END
```

```
// FOR MORIN
*NONPROCESS PROGRAM
*ONE WORD INTEGERS
*LIST ALL
*PUNCH
      SUBROUTINE MORIN(EL,C,ZLAM,EPS,I)
C
      DATA NR/2/
C
C     CHECK FIRST CARD FOR BLANK OR BAD INTEGER CODE
      READ (NR,2015) K,VAL
      IF (K)  60,60,1
    1 IF (5-K)  60,60,5
C
C     CHECK SUBSEQUENT CARD(S).
    2 READ (NR,2015) K,VAL
      IF (K)  50,50,3
    3 IF (5-K)  50,50,5
C
C     IF O.K. CODE GO TO MODIFY CORRESPONDING INPUT.
    5 GO TO (10,20,30,40),K
   10 EL  =VAL
      GO TO 2
   20 C   =VAL
      GO TO 2
   30 ZLAM=VAL
      GO TO 2
   40 EPS =VAL
      GO TO 2
C
C     END OF CHANGE CARDS, RETURN W/ FLAG SET TO RUN AGAIN.
   50 I=0
      RETURN
C     FIRST CARD BLANK, END OF CASE.
   60 I=1
      RETURN
C
 2015 FORMAT(I1,E14.7)
      END
```

```
// FOR EPFUN
*NONPROCESS PROGRAM
*ONE WORD INTEGERS
*LIST ALL
*PUNCH
      SUBROUTINE EPFUN(E,E1,E2,E3,E4)
      IF(E) 1,1,2
    1 E1=1.0
      E2=1.0
      E3=0.0
      E4=0.0
      GO TO 3
    2 EE=E*E
      EEE=EE*E
      EM=1.0-EE
      ES=SQRT (EM)
      ES3=ES*EM
      E2=2.0/EE*(1.0-ES)
      E1=E2/ES
      E4=(1.0-ES3)*2.0
      E5=2.0/EEE/ES3
      E3=E5*(3.0*EE-E4)
      E4=E5*(EE*(EE-3.0)+E4)
    3 RETURN
      END
```

```
// FOR KCEFG
*NONPROCESS PROGRAM
*ONE WORD INTEGERS
*LIST ALL
*PUNCH
      SUBROUTINE KCEFG(FR,PLAM,ALOD,FP,FM,FO,GP,GM,GO,AK1,AC1,AK2,AC2)
      K= -1
      P=PLAM
    3 P2=1.0+P*P
      PS=SQRT (P2)
      PF= P/P2
      AL=0.5*(PS+1.0)
      BE=0.5*(PS-1.0)
      BE= SQRT (BE)
      AL=SQRT (AL)
      IF(P) 1,1,2
    1 BE=-BE
    2 ABP=AL-BE*P
      APB=AL*P+BE
      IF(ALOD-100.0) 7,8,8
    7 PS=ALOD*PS
      ARG1=2.0*AL*ALOD
      ARG2=2.0*BE*ALOD
      E=EXP (ARG1)
      SH=0.5*(E-1.0/E)
      CH=0.5*(E+1.0/E)
      SF=SIN (ARG2)
      CF=COS (ARG2)
      DEN=PS*(CH+CF)
    8 XF=PF*P
      XG=-PF
      IF(ALOD-100.0) 9,10,10
    9 XF=PF*(ABP*SF-APB*SH)/DEN+XF
      XG= PF*(ABP*SH+APB*SF)/DEN+XG
   10 IF(K) 4,5,6
    4 FO=XF
      GO=-XG
      K=0
      P=PLAM*(1.0+2.0*FR)
      GO TO 3
    5 FP=XF
      GP=-XG
      K=1
      P=PLAM*(1.0-2.0*FR)
      GO TO 3
    6 FM=XF
      GM=-XG
      AK1=0.5*(FM+FP)
      AC1=-0.5*(GM-GP)
      AK2=0.5*(GM+GP)
      AC2=0.5*(FM-FP)
      RETURN
      END
```

INFLUENCE OF MAGNETIC FORCES
(UNIDIRECTIONAL OR BY AN ACTIVE DEVICE)
ON STABILITY OF PLAIN JOURNAL BEARING

SAMPLE PRODUCTION RUN JUNE 1969

L	C	MU	P-SUB-A	D
.1 00 00 -0 1	.20 00 0-02	.2 70 00 -0 8	.14 70 0+ 02	.3 50 00 +0 1
E-SUB-A	E-SUB-B	DELTA-E		
.3 60 00 -0 0	.40 00 0-00	.2 00 00 -0 1		

LAMBDA	EPSILON	CAP-L/D
.1 07 00 +0 1	.38 70 0-00	.1 00 00 +0 1

MODE	MDIAG	MP	MACT
2	0	-1	1

AU-XX	AU-XY	AU-YX	AU-YY
.2 00 00	.00000	.0 00 00	.00 00 0

AV-XX	AV-XY	AV-YX	AV-YY
.3 00 00 -0 1	.00000	.0 00 00	.3 00 0 0-01

OMEGA
.1 25 81 +0 4

F = .3600-00

W-SUB-XO	W-SUB-YO	ALPHA	F-BAR
-.15433-01	.46981-01	.71815+02	.49451-01

F-SUB-M	K-SUB-M	K-SUB-MX	K-SUB-MY
.27976+02	.10700-01	-.61733-02	-.18792-01

FORCE COEFFICIENTS WITH MAGNETIC FORCES GENERATED BY AN ACTIVE DEVICE

U-XX	U-XY	U-YX	U-YY
.62524-01	.10684+00	-.11823+00	.51175-01

V-XX	V-XY	V-YX	V-YY
.10709+00	-.48732-01	.44934-01	.10108+00

A	B	ZR	ZY
-.41674-01	.42385-01	-.94252-01	-.22485-00

W(F) = -.16682-01

F = .38000-00

W-SUB-XO	W-SUB-YO	ALPHA	F-BAR
-.15433-01	.46981-01	.71815+02	.49451-01

F-SUB-W	K-SUB-M	K-SUB-MX	K-SUB-MY
.27976+02	-.19780-01	-.61733-02	-.18792-01

FORCE COEFFICIENTS WITH MAGNETIC FORCES GENERATED BY AN ACTIVE DEVICE

U-XX	U-XY	U-YX	U-YY
.63910-01	.10528+00	-.11679+00	.52453-01
V-XX	**V-XY**	**V-YX**	**V-YY**
.11118+00	-.51014-01	.47039-01	.10485+00
A	**B**	**ZR**	**ZI**
-.39493-01	.43786-01	-.98672-01	-.22188-00

W(F) = -.59465-02

F = .40000-00

W-SUB-XO	W-SUB-YO	ALPHA	F-BAR
-.15433-01	.46981-01	.71815+02	.49451-01

F-SUB-W	K-SUB-M	K-SUB-MX	K-SUB-MY
.27976+02	-.19780-01	-.61733-02	-.18792-01

FORCE COEFFICIENTS WITH MAGNETIC FORCES GENERATED BY AN ACTIVE DEVICE

U-XX	U-XY	U-YX	U-YY
.65368-01	.10366+00	-.11530+00	.53797-01
V-XX	**V-XY**	**V-YX**	**V-YY**
.11529+00	-.53233-01	.49085-01	.10859+00

A	B	ZR	ZI
-.37264-01	.45056-01	-.10297+00	-.21878-00

W(F) = .50456-02

F = .39074-00

W-SUB-XO	W-SUB-YO	ALPHA	F-BAR
-.15433-01	.46981-01	.71815+02	.49451-01
F-SUB-M	K-SUB-M	K-SUB-MX	K-SUB-MY
.27976+02	.13760-01	-.61733-02	-.18792-01

FORCE COEFFICIENTS WITH MAGNETIC FORCES GENERATED BY AN ACTIVE DEVICE

U-XX	U-XY	U-YX	U-YY
.64684-01	.10442+00	-.11600+00	.53166-01
V-XX	V-XY	V-YX	V-YY
.11336+00	-.52213-01	.48144-01	.10686+00
A	B	ZR	ZI
-.38302-01	.44484-01	-.10099+00	-.22023-00

W(F) = -.65137-05

M	CAP-M	T.S.
.55202-01	.37478+01	.10566+01

EXIT CALLED AT LOCATION 015526

APPENDIX IV: STABILIZATION WITH QUADRATIC DAMPING

SPECIAL SYMBOLS FOR APPENDIX IV

Note: The unit is dimensionless unless otherwise indicated in brackets.

C radial bearing clearance [in.]

D bearing diameter [in.]

$\mathscr{E}$ dimensionless work per cycle dissipated by virtual damping

f Ω/ω, frequency ratio

L bearing length [in.]

M rotor mass [lb-sec^2/in.]

m $MC\omega^2/(p_a \pi LD)$, dimensionless rotor mass

n harmonic number of the shaft center orbit

p_a ambient pressure [psia]

t time [sec.]

$\left\{\begin{matrix} U_{xxn} \\ U_{xyn} \end{matrix}\right\}$ peak amplitude of the in-phase component of W_{xt} in response to the nth harmonic of the $\left\{\begin{matrix} x \\ y \end{matrix}\right\}$ component of the shaft center orbit

$\left\{\begin{matrix} U_{yxn} \\ U_{yyn} \end{matrix}\right\}$ peak amplitude of the in-phase component of W_{yt} in response to the nth harmonic of the $\left\{\begin{matrix} x \\ y \end{matrix}\right\}$ component of the shaft center orbit

$\left\{\begin{matrix} U_{/\!/n} \\ V_{/\!/n} \\ U_{\angle n} \\ V_{\angle n} \end{matrix}\right\}$ $\left\{\begin{matrix} U_{xxn} = U_{yyn} \\ V_{xxn} = V_{yyn} \\ U_{xyn} = -U_{yxn} \\ V_{xyn} = -V_{yxn} \end{matrix}\right\}$ for $\epsilon_{xo} = 0$

$\left\{\begin{matrix} u_{xn} \\ v_{xn} \end{matrix}\right\}$ Fourier coefficient of $\left\{\begin{matrix} \cos nf\tau \\ \sin nf\tau \end{matrix}\right\}$ of $(W_{xt})_m$

$\left\{\begin{matrix} u_{yn} \\ v_{yn} \end{matrix}\right\}$ Fourier coefficient of $\left\{\begin{matrix} \cos nf\tau \\ \sin nf\tau \end{matrix}\right\}$ of $(W_{yt})_m$

V_{xxn}, V_{xyn} — peak amplitude of the quadrature component of W_{xt} in response to the nth harmonic of the $\begin{Bmatrix} x \\ y \end{Bmatrix}$ component of the shaft center orbit

V_{yxn}, V_{yyn} — peak amplitude of the quadrature component of W_{yt} in response to the nth harmonic of the $\begin{Bmatrix} x \\ y \end{Bmatrix}$ component of the shaft center orbit

W_{xt}, W_{yt} — dimensionless time dependent bearing forces respectively in x and y directions

$(W_{xt})_m, (W_{yt})_m$ — dimensionless time dependent bearing forces of the electromagnets respectively in x and y directions

β — dimensionless virtual damping coefficient

β_m — dimensionless coefficient of the damping force of the electromagnets

ϵ_1 — $\epsilon_{xt1} = \epsilon_{yt1}$ for $\epsilon_{xo} = 0$

ϵ_{xo} — static portion of ϵ_x

ϵ_{xtn} — peak amplitude of the nth harmonic of the x component of the dimensionless shaft center orbit

ϵ_{ytn} — peak amplitude of the nth harmonic of the y component of the dimensionless shaft center orbit

ϵ_x, ϵ_y — dimensionless shaft center displacements respectively in x and y directions

Λ — compressibility number of gas bearing

τ — ωt, dimensionless time

ω — shaft rotational speed [radian/sec.]

φ_n — $\varphi_{xn} = \varphi_{yn} + \pi/2$ for $\epsilon_{xo} = 0$

φ_{xn} — phase angle of the nth harmonic of the x component of the shaft center orbit [radians]

φ_{yn}	phase angle of the nth harmonic of the y component of the shaft center orbit [radians]
Ω	fundamental orbit frequency of shaft center [radians/sec.]

The stability analysis cited in Section II and Appendix I is applicable only to linear systems, and therefore it is not capable of coping with the concept proposed in Section III B, in which electro-magnets would be used to impose quadratic damping forces on the shaft. In this Appendix, a more general criterion to determine the stability of the shaft-bearing system will be derived. The more general criterion is based on the concept of "virtual damping for a stationary state".

Consider the dynamic equilibrium amongst the virtual damping force, the D'alembert force of the shaft, and the bearing force and the force of the electro-magnet in the dimensionless form:

$$-\beta \frac{d\epsilon_x}{d\tau} - m \frac{d^2\epsilon_x}{d\tau^2} + W_{xt} + (W_{xt})_m = 0 \qquad \text{(IV.1a)}$$

$$-\beta \frac{d\epsilon_y}{d\tau} - m \frac{d^2\epsilon_y}{d\tau^2} + W_{yt} + (W_{yt})_m = 0 \qquad \text{(IV.1b)}$$

β is the "virtual damping coefficient" (written non-dimensionally). It is assumed, that with the introduction of the virtual damping, the system would sustain a state of periodic motion such that

$$\left.\begin{aligned} \epsilon_x\ (\tau = 2\pi/f) &= \epsilon_x\ (\tau = 0) \\ \epsilon_y\ (\epsilon = 2\pi/f) &= \epsilon_y\ (\tau = 0) \end{aligned}\right\} \qquad \text{(IV.2)}$$

The energy dissipated by the virtual damping per cycle of the periodic motion is obtained by multiplying $d\epsilon_x/d\tau$ and $d\epsilon_y/d\tau$ into Eqs. (IV.1a) and (IV.1b) then integrating over one period:

$$\mathcal{E} = \int_0^{2\pi/f} \beta \left[\left(\frac{d\epsilon_x}{d\tau}\right)^2 + \left(\frac{d\epsilon_y}{d\tau}\right)^2 \right] d\tau$$

$$= -m \int_0^{2\pi/f} \left(\frac{d^2\epsilon_x}{d\tau^2} \frac{d\epsilon_x}{d\tau} + \frac{d^2\epsilon_y}{d\tau^2} \frac{d\epsilon_y}{d\tau} \right) d\tau$$

$$+ \int_0^{2\pi/f} \left[\left\{ W_{xt} + (W_{xt})_m \right\} \frac{d\epsilon_x}{d\tau} + \left\{ W_{yt} + (W_{yt})_m \right\} \frac{d\epsilon_y}{d\tau} \, d\tau \right]$$

Since $\frac{d^2\epsilon_x}{d\tau^2} \frac{d\epsilon_x}{d\tau} d\tau = \frac{1}{2} d \left(\frac{d\epsilon_x}{d\tau}\right)^2$ and $\frac{d^2\epsilon_y}{d\tau^2} \frac{d\epsilon_y}{d\tau} d\tau = \frac{1}{2} d \left(\frac{d\epsilon_y}{d\tau}\right)^2$ and since the periodic condition applies to $\frac{d\epsilon_x}{d\tau}$ and $\frac{d\epsilon_y}{d\tau}$ as well

$$m \int_0^{2\pi/f} \left(\frac{d^2\epsilon_x}{d\tau^2} \frac{d\epsilon_x}{d\tau} + \frac{d^2\epsilon_y}{d\tau^2} \frac{d\epsilon_y}{d\tau} \right) d\tau = 0$$

Clearly, this simply indicates that the D'alembert forces would alternately store and release energy during different parts of the period, but would have no net contribution to the energy of the system when the entire period is considered. Thus

$$\beta = \frac{\mathcal{E}^0}{\int_0^{2\pi/f} \left[\left(\frac{d\epsilon_x}{d\tau}\right)^2 + \left(\frac{d\epsilon_y}{d\tau}\right)^2 \right] d\tau}$$

$$= \frac{\int_0^{2\pi/f} \left[\left\{ W_{xt} + (W_{xt})_m \right\} \frac{d\epsilon_x}{d\tau} + \left\{ W_{yt} + (W_{yt})_m \right\} \frac{d\epsilon_y}{d\tau} \right] d\tau}{\int_0^{2\pi/f} \left[\left(\frac{d\epsilon_x}{d\tau}\right)^2 + \left(\frac{d\epsilon_y}{d\tau}\right)^2 \right] d\tau} \qquad \text{(IV.3)}$$

If β is zero, the prescribed motion (ϵ_x, ϵ_y) defines a stationary state of periodic motion. If β is positive, implying the need of additional damping to sustain the prescribed motion, the system is unstable; and if β is negative, conversely, the system is stable.

In general, one must permit the periodic motion to contain harmonic components, e.g:

$$\left.\begin{aligned} \epsilon_x &= \epsilon_{xo} + \Sigma\, \epsilon_{xtn} \cos\,(nf\tau - \varphi_{xn}) \\ \epsilon_y &= \Sigma\, \epsilon_{ytn} \cos\,(nf\tau - \varphi_{yn}) \end{aligned}\right\} \qquad \text{(IV.4)}$$

Coupling between the two degrees of freedom, x and y, is usually imposed through the bearing forces, W_{xt} and W_{yt}, both of which generally depend on both ϵ_x and ϵ_y.

Assuming that ϵ_{xtn} and ϵ_{ytn} are small enough so that the orbit amplitude is small in comparison with the bearing film thickness, then, consistent with Equation (IV.4), the dynamic bearing forces can be expressed as:

$$\left.\begin{aligned} W_{xt} &= -\Sigma\Big\{\big[U_{xxn} \cos\,(nf\tau - \varphi_{xn}) - V_{xxn} \sin\,(nf\tau - \varphi_{xn})\big]\epsilon_{xtn} \\ &\quad + \big[U_{xyn} \cos\,(nf\tau - \varphi_{yn}) - V_{xyn} \sin\,(nf\tau - \varphi_{yn})\big]\epsilon_{ytn}\Big\} \\ W_{yt} &= -\Sigma\Big\{\big[U_{yxn} \cos\,(nf\tau - \varphi_{xn}) - V_{yxn} \sin\,(nf\tau - \varphi_{xn})\big]\epsilon_{xtn} \\ &\quad + \big[U_{yyn} \cos\,(nf\tau - \varphi_{yn}) - V_{yyn} \sin\,(nf\tau - \varphi_{yn})\big]\epsilon_{ytn}\Big\} \end{aligned}\right\} \qquad \text{(IV.5)}$$

U_{xxn}, V_{xxn}, U_{xyn}, V_{xyn}, U_{yxn}, V_{yxn}, U_{yyn}, and V_{yyn} are solutions of the dynamically perturbed gas lubrication equation and are generally dependent on the bearing geometry, Λ, ϵ_{xo}, and nf.

The relative magnitudes of ϵ_{xtn} and ϵ_{ytn} as well as the relative phase angles φ_{xn} and φ_{yn} must satisfy Equations (IV.1a) and (IV.1b) and make β most positive (so that the system may select its own orbit to become unstable). The forces of the electromagnets described in Section IIIB according to Equations (52) and (53) can be expressed as:

$$\left.\begin{aligned}(W_{xt})_m &= -\beta_m \left|\frac{d\epsilon_x}{d\tau}\right| \frac{d\epsilon_x}{d\tau} \\ (W_{yt})_m &= -\beta_m \left|\frac{d\epsilon_y}{d\tau}\right| \frac{d\epsilon_y}{d\tau}\end{aligned}\right\} \qquad \text{(IV.6)}$$

β_m is a coefficient determined by the circuit design.

It is not possible to evaluate Equations (IV.6) when the coefficients in Equation (IV.4) are not yet determined. Therefore, one must begin with the approximation:

$$\left.\begin{aligned}\epsilon_x &= \epsilon_{xo} + \epsilon_{xt1} \cos(f\tau) \\ \epsilon_y &= \epsilon_{yt1} \cos(f\tau - \varphi_{y1})\end{aligned}\right\} \qquad \text{(IV.7)}$$

and seek the harmonic terms in an iterative manner.

For an example, consider

$$\epsilon_{xo} = 0 \tag{IV.8}$$

consequently, due to symmetry,

$$\left.\begin{aligned} U_{xxn} &= U_{yyn} = U_{/\!/n} \\ V_{xxn} &= V_{yyn} = V_{/\!/n} \\ U_{xyn} &= -U_{yxn} = U_{\not/n} \\ V_{xyn} &= -V_{yxn} = V_{\not/n} \end{aligned}\right\} \tag{IV.9}$$

which are dynamic perturbation solutions corresponding to the frequency of the unloaded plain journal bearing cited in Appendix I and [Ref. 5]. Thus,

$$\left.\begin{aligned} W_{xt} &= -\left[(U_{/\!/1}\cos f\tau - V_{/\!/1}\sin f\tau)\right]\epsilon_{xt1} \\ &\quad -\left[(U_{\not/1}\cos(f\tau - \omega_{y1}) - V_{\not/1}\sin(f\tau - \omega_{y1})\right]\epsilon_{yt1} \\ W_{yt} &= \left[U_{\not/1}\cos f\tau - V_{\not/1}\sin f\tau\right]\epsilon_{xt1} \\ &\quad -\left[U_{/\!/1}\cos(f\tau - \omega_{y1}) - V_{/\!/1}\sin(f\tau - \omega_{y1})\right]\epsilon_{yt1} \end{aligned}\right\} \tag{IV.10}$$

Differentiating Equations (IV.7) with respect to τ:

$$\left.\begin{aligned} \frac{d\epsilon_x}{d\tau} &= -f\,\epsilon_{xt1}\sin f\tau \\ \frac{d\epsilon_y}{d\tau} &= -f\,\epsilon_{yt1}\sin(f\tau - \omega_{y1}) \end{aligned}\right\} \tag{IV.11}$$

Consequently,

$$\int_0^{2\pi/f} \left[\left(\frac{d\epsilon_x}{d\tau} \right)^2 + \left(\frac{d\epsilon_y}{d\tau} \right)^2 \right] d\tau = \pi f \left(\epsilon_{xt1}^2 + \epsilon_{yt1}^2 \right) \qquad \text{(IV.12)}$$

$$\int_0^{2\pi/f} \left(W_{xt} \frac{d\epsilon_x}{d\tau} + W_{yt} \frac{d\epsilon_y}{d\tau} \right) d\tau$$

$$= -\pi \left[V_{//1} \left(\epsilon_{xt1}^2 + \epsilon_{yt1}^2 \right) - 2U_{\angle 1} \sin \varphi_{y1} \, \epsilon_{xt1} \, \epsilon_{yt1} \right] \qquad \text{(IV.13)}$$

$$\int_0^{2\pi/f} \left\{ (W_{xt})_m \frac{d\epsilon_x}{d\tau} + (W_{yt})_m \frac{d\epsilon_y}{d\tau} \right\} d\tau$$

$$= -\beta_m \int_0^{2\pi/f} \left[\left| \frac{d\epsilon_x}{d\tau} \right|^3 + \left| \frac{d\epsilon_y}{d\tau} \right|^3 \right] d\tau$$

$$= -\frac{8}{3} \beta_m f^2 \left(\epsilon_{xt1}^3 + \epsilon_{yt1}^3 \right) \qquad \text{(IV.14)}$$

Now, substitute Equations (IV.12), (IV.13), and (IV.14) into Equation (IV.3), and one finds:

$$\left.\begin{aligned} \beta = -\frac{1}{f} \left[V_{//n} - \frac{2\epsilon_{xt1} \epsilon_{yt1}}{\epsilon_{xt}^2 + \epsilon_{yt}^2} \sin \varphi_{y1} \, U_{\angle 1} \right] \\ - \frac{8}{3\pi} \beta_m f \left(\frac{\epsilon_{xt1}^3 + \epsilon_{yt1}^3}{\epsilon_{xt1}^2 + \epsilon_{yt1}^2} \right) \end{aligned}\right\} \qquad \text{(IV.15)}$$

To make β most positive, one finds

$$\epsilon_{xt1} = \epsilon_{yt1} = \epsilon_1 \tag{IV.16}$$

and

$$\sin \omega_{y1} = sg\left(U_{\perp 1}\right)$$

Actually, since $U_{\perp 1}$ is always positive according to numerical results, one simply has

$$\omega_{y1} = \frac{\pi}{2} \tag{IV.17}$$

Thus,

$$\beta = \frac{1}{f}\left[-V_{/\!/1} + U_{\perp 1}\right] - \frac{8}{3\pi}\beta_m f \epsilon_1 \tag{IV.18}$$

At the stationary state, $\beta = 0$, then

$$(\epsilon_1)_{stationary} = \frac{3\pi}{8}\frac{(U_{\perp 1} - V_{/\!/1})}{\beta_m f^2} \tag{IV.19}$$

If $\epsilon_1 < (\epsilon_1)_{stationary}$, β would be positive, then the system is unstable, and ϵ_1 would grow. If $\epsilon_1 > (\epsilon_1)_{stationary}$, β would be negative, and ϵ_1 would diminish. Thus the presence of $(W_{xt})_m$ and $(W_{yt})_m$ stabilizes the orbit size at ϵ_1, which, however, can not be completely reduced to zero. To determine f, substitute Equations (IV.6), (IV.7), (IV.10), (IV.11), (IV.16), (IV.17) and $\beta = 0$ into

Equation (IV.1a):

$$
\begin{aligned}
& mf^2 \cos f\tau - U_{//1} \cos f\tau \\
& + V_{//1} \sin f\tau - U_{\perp 1} \sin f\tau - V_{\perp 1} \cos f\tau \\
& + \beta_m f^2 \varepsilon_1 \left|\sin f\tau\right| \sin f\tau \\
= & - \sin f\tau \left[U_{\perp 1} - V_{//1} - \beta_m f^2 \varepsilon_1 \left|\sin f\tau\right| \right] \\
& - \cos f\tau \left[U_{//1} + V_{\perp 1} - mf^2 \right] \\
\approx & \quad 0 \qquad\qquad (IV.20)
\end{aligned}
$$

One should note that the last expression cannot be precisely zero because the truncated description of the periodic motion is only an approximation. Also, Eq. (IV.1b) needs not be separately considered because of the prevailing symmetry. Since, even and odd functions of τ should separately vanish in the above expression, one would find

$$f = \sqrt{\frac{U_{//1} + V_{\perp 1}}{m}} \qquad (IV\ 21)$$

Harmonic contents in the motion of the stationary state can be obtained from Eqs. (IV.1 a,b) by performing a Fourier analysis in an iterative manner beginning with the truncated expressions, Eq. (IV.7), as the initial guess in the non-linear terms, which are defined by Eq. (IV.6). The iterative procedure may be continued to improve accuracy further. The process begins with finding the harmonic contents of Eq. (IV.6) by the substitution of Eqs. (IV.11), (IV.16) and (IV.17) and then performing the appropriate Fourier analysis.

$$(W_{xt})_m = \sum_{n=1}^{\infty} (u_{xn} \cos nf\tau + v_{xn} \sin nf\tau)$$

$$(W_{yt})_m = \sum_{n=1}^{\infty} (u_{yn} \cos nf\tau + v_{yn} \sin nf\tau) \qquad \text{(IV.22)}$$

$$\left.\begin{aligned}
u_{xn} &= \beta_m \frac{f}{\pi} \int_0^{2\pi/f} \left|\frac{d\epsilon_x}{d\tau}\right| \frac{d\epsilon_x}{d\tau} \cos nf\tau \, d\tau \\
v_{xn} &= \beta_m \frac{f}{\pi} \int_0^{2\pi/f} \left|\frac{d\epsilon_x}{d\tau}\right| \frac{d\epsilon_x}{d\tau} \sin nf\tau \, d\tau \\
u_{yn} &= \beta_m \frac{f}{\pi} \int_0^{2\pi/f} \left|\frac{d\epsilon_y}{d\tau}\right| \frac{d\epsilon_y}{d\tau} \cos nf\tau \, d\tau \\
v_{yn} &= \beta_m \frac{f}{\pi} \int_0^{2\pi/f} \left|\frac{d\epsilon_y}{d\tau}\right| \frac{d\epsilon_y}{d\tau} \sin nf\tau \, d\tau
\end{aligned}\right\} \qquad \text{(IV.23)}$$

Or, with the aid of Eqs. (IV.11) and (IV.17)

$$u_{x1} \approx \beta_m \frac{f^3 \epsilon_1^2}{\pi} \int_0^{2\pi/f} |\sin f\tau| \sin f\tau \cos f\tau \, d\tau = 0$$

$$v_{x1} \approx \beta_m \frac{f^3 \epsilon_1^2}{\pi} \int_0^{2\pi/f} |\sin f\tau| \sin^2 f\tau \, d\tau = \frac{8\beta_m}{3\pi} f^2 \epsilon_1^2$$

$$u_{x2} \approx \beta_m \frac{f^3 \epsilon_1^2}{\pi} \int_0^{2\pi/f} |\sin f\tau| \sin f\tau \cos 2f\tau = 0$$

$$v_{x2} \approx \beta_m \frac{f^3 \epsilon_1^2}{\pi} \int_0^{2\pi/f} |\sin f\tau| \sin f\tau \sin 2f\tau \, d\tau = 0$$

$$u_{xn} \approx 0 \quad \text{for all } n$$

$$v_{xn} \approx 0 \quad \text{for all even } n$$

$$v_{xn} \approx \frac{8\beta_m}{n(n^2-4)\pi} f^2 \epsilon_1^2 \quad \text{for all odd } n$$

(IV.24a)

$$u_{y1} \approx -\beta_m \frac{f^3 \epsilon_1^2}{\pi} \int_0^{2\pi/f} |\cos f\tau| \cos^2 f\tau \, d\tau = -\frac{8\beta_m}{3\pi} f^2 \epsilon_1^2$$

$$v_{y1} \approx -\beta_m \frac{f^2 \epsilon_1^2}{\pi} \int_0^{2\pi/f} |\cos f\tau| \cos f\tau \sin f\tau \, d\tau = 0$$

$$u_{yn} \approx 0 \quad \text{for all even } n$$

$$u_{yn} \approx \frac{8\beta_m}{n(n^2-4)\pi} f^2 \epsilon_1^2 \quad \text{for all odd } n$$

$$v_{yn} \approx 0 \quad \text{for all } n$$

(IV.24b)

Substituting Eqs. (IV.4), (IV.5), (IV.9), and (IV.22) into Eq. (IV.1a) and (IV.1b), setting $\beta = 0$ for the stationary state:

$$m \sum_{n=1}^{\infty} n^2 f^2 \epsilon_{xtn} \cos (nf\tau - \varphi_{xn})$$

$$- \sum_{n=1}^{\infty} \left\{ \epsilon_{xtn} \left[U_{//n} \cos (nf\tau - \varphi_{xn}) - V_{//n} \sin (nf\tau - \varphi_{xn}) \right] \right.$$

$$\left. + \epsilon_{ytn} \left[U_{\angle n} \cos (nf\tau - \varphi_{yn}) - V_{\angle n} \sin (nf\tau - \varphi_{yn}) \right] \right\}$$

$$+ \sum_{n=1}^{\infty} (u_{xn} \cos nf\tau + v_{xn} \sin nf\tau)$$

$$= - \sum_{n=1}^{\infty} \left\{ \cos nf\tau \left[(\beta nf \sin \varphi_{xn} - m n^2 f^2 \cos \varphi_{xn} + U_{//n} \cos \varphi_{xn} + V_{//n} \sin \varphi_{xn}) \epsilon_{xtn} \right. \right.$$

$$\left. + (U_{\angle n} \cos \varphi_{yn} + V_{\angle n} \sin \varphi_{yn}) \epsilon_{ytn} - u_{xn} \right]$$

$$+ \sin nf\tau \left[(-\beta nf \cos \varphi_{xn} - mn^2 f^2 \sin \varphi_{xn} + U_{//n} \sin \varphi_{xn} - V_{//n} \cos \varphi_{xn}) \epsilon_{xtn} \right.$$

$$\left. \left. + (U_{\angle n} \sin \varphi_{yn} - V_{\angle n} \cos \varphi_{yn}) \epsilon_{ytn} - v_{xn} \right] \right\}$$

$$= 0$$

Or,

$$\left.\begin{aligned}
&\left[(m\,n^2f^2 - U_{//n})\cos\varphi_{xn} - V_{//n}\sin\varphi_{xn}\right]\epsilon_{xtn} \\
&\qquad - (U_{\angle n}\cos\varphi_{yn} + V_{\angle n}\sin\varphi_{yn})\,\epsilon_{ytn} = -u_{xn} \\
&\left[(m\,n^2f^2 - U_{//n})\sin\varphi_{xn} + V_{//n}\cos\varphi_{xn}\right]\epsilon_{xtn} \\
&\qquad - (U_{\angle n}\sin\varphi_{yn} - V_{\angle n}\cos\varphi_{yn})\,\epsilon_{ytn} = -v_{xn}
\end{aligned}\right\} \qquad \text{(IV.25a)}$$

and similarly,

$$\left.\begin{aligned}
&\left[(m\,n^2f^2 - U_{//n})\cos\varphi_{yn} - V_{//n}\sin\varphi_{yn}\right]\epsilon_{ytn} \\
&\qquad + (U_{\angle n}\cos\varphi_{xn} + V_{\angle n}\sin\varphi_{xn})\,\epsilon_{xtn} = -u_{yn} \\
&\left[(m\,n^2f^2 - U_{//n})\sin\varphi_{yn} + V_{//n}\cos\varphi_{yn}\right]\epsilon_{ytn} \\
&\qquad + (U_{\angle n}\sin\varphi_{xn} - V_{\angle n}\cos\varphi_{xn})\,\epsilon_{xtn} = -v_{yn}
\end{aligned}\right\} \qquad \text{(IV.25b)}$$

It is not necessary to consider Eqs. (IV.25) with n = 1 since these conditions would be consistent with Eqs. (IV.7), (IV.16), (IV.17), and (IV.19). For n = an even integer, because $u_{xn} = u_{yn} = v_{xn} = v_{yn} = 0$, one also must have $\epsilon_{xtn} = \epsilon_{ytn} = 0$. For n = an odd integer, Eqs. (IV.25) can be rewritten into the following matrix form:

$$\begin{bmatrix} m n^2 f^2 - U_{//n} & -V_{//n} & -U_{\angle n} & -V_{\angle n} \\ V_{//n} & m n^2 f^2 - U_{//n} & V_{\angle n} & -U_{\angle n} \\ U_{\angle n} & V_{\angle n} & m n^2 f^2 - U_{//n} & -V_{//n} \\ -V_{\angle n} & U_{\angle n} & V_{//n} & m n^2 f^2 - U_{//n} \end{bmatrix} \begin{bmatrix} \epsilon_{xtn} \cos \omega_{xn} \\ \epsilon_{xtn} \sin \omega_{xn} \\ \epsilon_{ytn} \cos \omega_{yn} \\ \epsilon_{ytn} \sin \omega_{yn} \end{bmatrix}$$

$$= \begin{bmatrix} 0 \\ \frac{8\beta_m}{n(n^2-4)\pi} f^2 \epsilon_1^2 \\ -\frac{8\beta_m}{n(n^2-4)\pi} f^2 \epsilon_1^2 \\ 0 \end{bmatrix} \qquad \text{(IV.26)}$$

Solving,

$$\epsilon_{xtn} \cos \omega_{xn} = \epsilon_{ytn} \sin \omega_{yn}$$

$$= \frac{(V_{//n} - U_{\angle n})}{(m n^2 f^2 - U_{//n} - V_{\angle n})^2 + (V_{//n} - U_{\angle n})^2} \frac{8\beta_m}{n(n^2-4)\pi} f^2 \epsilon_1^2$$

$$\epsilon_{xyn} \sin \omega_{xn} = -\epsilon_{ytn} \cos \omega_{yn}$$

$$= \frac{(m n^2 f^2 - U_{//n} - V_{\angle n})}{(m n^2 f^2 - U_{//n} - V_{\angle n})^2 + (V_{//n} - U_{\angle n})^2} \frac{8\beta_m}{n(n^2-4)\pi} f^2 \epsilon_1^2$$

Or,

$$\varphi_{xn} = \varphi_{yn} - \pi/2$$

$$= \tan^{-1} \frac{(m\, n^2 f^2 - U_{//n} - V_{//n})}{(U_{\perp n} - V_{//n})} \qquad \text{(IV.27)}$$

and by virtue of Eq. (IV.19),

$$\epsilon_{xtn} = \epsilon_{ytn}$$

$$= \frac{3\epsilon_1}{n(4-n^2)} \frac{(U_{\perp 1} - V_{//1})}{\sqrt{(m\, n^2 f^2 - U_{//n} - V_{\perp n})^2 + (U_{\perp n} - V_{//n})^2}} \qquad \text{(IV.28)}$$

These two formulae are valid for all positive odd integers, including n = 1. In principle, additional iterations can be performed.

Summarizing, according to the one-step iteration analysis carried out above, an unloaded, plain journal bearing-shaft system would be stabilized by the electromagnets to assume a "steady-state" orbit. Collecting the relevant formulae, Eqs. (IV.21), (IV.19), (IV.27), and (IV.28) and rearranging somewhat for clearer presentation, the "steady-state" orbit can be described as follows:

$$\left.\begin{aligned} \epsilon_x &= -\frac{3\pi}{8}\left(\frac{U_{\perp 1} - V_{//1}}{U_{//1} + V_{\perp 1}}\right)\frac{m}{\beta_m} \sum_{n=1,3,5\cdots} \frac{3}{n(4-n^2)} \frac{(U_{\perp 1} - V_{//1})\cos(nf\tau - \varphi_n)}{\sqrt{(m\, n^2 f^2 - U_{//n} - V_{\perp n})^2 + (U_{\perp n} - V_{//n})^2}} \\ \epsilon_y &= -\frac{3\pi}{8}\left(\frac{U_{\perp 1} - V_{//1}}{U_{//1} + V_{\perp 1}}\right)\frac{m}{\beta_m} \sum_{n=1,3,5\cdots} \frac{3}{n(4-n^2)} \frac{(U_{\perp 1} - V_{//1})\sin(nf\tau - \varphi_n)}{\sqrt{(m\, n^2 f^2 - U_{//n} - V_{\perp n})^2 + (U_{\perp n} - V_{//n})^2}} \end{aligned}\right\} \qquad \text{(IV.29)}$$

where,

$$\left.\begin{aligned} \varphi_n &= \tan^{-1}\left(\frac{m\,n^2 f^2 - U_{//n} - V_{/n}}{U_{\perp n} - V_{//n}}\right) \\ f &= \sqrt{\frac{U_{//1} + V_{\perp 1}}{m}} \\ \begin{bmatrix} U_{//n} \\ V_{//n} \\ U_{\perp n} \\ V_{\perp n} \end{bmatrix} &= \begin{bmatrix} U_{//}(nf) \\ V_{//}(nf) \\ U_{\perp}(nf) \\ V_{\perp}(nf) \end{bmatrix} \end{aligned}\right\} \qquad \text{(IV.30)}$$

REFERENCES

1. Vohr, J. H. and Chow, C. Y., "Characteristics of Herringbone-Grooved, Gas-Lubricated Journal Bearings", Trans. ASME 64-LUB-15 Journal of Basic Engineering, Vol. 87, Ser. D. No. 3, Sept. 1965.

2. Pan, C.H.T., "Spectral Analysis of Gas Bearing Systems for Stability Studies", presented at the Ninth Midwestern Mechanics Conference, University of Wisconsin, Madison, Wis., Aug. 1965.

3. Malanoski, S. B., "Experiments on an Ultra-Stable Gas Journal Bearing", 66-LUB-6, presented at the ASME-ASLE Lubrication Conference, Minnesota, Oct. 18-20, 1966.

4. McHugh, J. D., "Magnetic Bearing Systems - A Comparison of Various Approaches", Proc. of USAF-SWRI Aerospace Bearing Conference, San Antonio, Texas, 1964.

5. Pan, C.H.T., and Malanoski, S. B., Discussion of "On the Behavior of Gas-Lubricated Journal Bearings Subjected to Sinusoidally Time-Varying Loads", by Ausman, J. S., Journal of Basic Engineering, Trans. ASME, Series D, Vol. 87, No. 3, Sept. 1965, pp. 599-603.

6. Dawes, C. L., "Electrical Engineering", Vol. I, McGraw-Hill Book Co., 1952, pp. 265-271.

7. Ausman, J. S., "Finite Gas-Lubricated Journal Bearing", The Institute of Mechanical Engineers, Proceedings of the Conference on Lubrication and Wear, 1957, pp. 39-45.

8. Savant, C. J., "Control System Design", McGraw-Hill Book Co., Second Ed., 1964, p. 239.

9. Cook, A. L. and Carr, C. C., "Elements of Electrical Engineering", Fifth Edition, John Wiley and Sons, Inc., 1947.

10. Pinkus, O. and Sternlicht, B., "Theory of Hydrodynamic Lubrication", McGraw-Hill Book Co., 1961.

11. Hutte, "Engineer's Handbook" (in German), Part IVB, Wilhelm Ernst & Co., Berlin, 1962, pp. 250-253.

12. Kamke, E., "Differential Equations", Chelsea Publishing Co., Third Edition, 1959.

13. Bozorth, R.M., "Ferromagnetism", Van Nostrand Co., 1951.

14. American Institute of Physics Handbook, Second Edition, McGraw-Hill Book Co., 1963.

Unclassified
Security Classification

DOCUMENT CONTROL DATA - R & D

(Security classification of title, body of abstract and indexing annotation must be entered when the overall report is classified)

Mechanical Technology Inc. 968 Albany Shaker Road Latham, New York 12110	2a. REPORT SECURITY CLASSIFICATION: Unclassified 2b. GROUP: NA

3. REPORT TITLE
Rotor-Bearing Dynamics Design Technology, Part X, Feasibility Study of Electromagnetic Means to Improve the Stability of Rotor-Bearing Systems

4. DESCRIPTIVE NOTES *(Type of report and inclusive dates)*
Final report summarizing effort from 1 May 1967 to 1 September 1968

5. AUTHOR(S) *(First name, middle initial, last name)*
T.Chiang

6. REPORT DATE	7a. TOTAL NO. OF PAGES	7b. NO. OF REFS
April, 1970	113	14

8a. CONTRACT OR GRANT NO.	9a. ORIGINATOR'S REPORT NUMBER(S)
b. PROJECT NO. 3048 c. Task No. 304806 d.	9b. OTHER REPORT NO(S) *(Any other numbers that may be assigned this report)* AFAPL-TR-65-45, Part X

10. DISTRIBUTION STATEMENT
This document is subject to special export controls and each transmittal to foreign governments or foreign nationals may be made only with the approval of AFAPL, Wright-Patterson AFB, Ohio 45433

11. SUPPLEMENTARY NOTES	12. SPONSORING MILITARY ACTIVITY
None	USAF AFSC - Aero Propulsion Laboratory Wright-Patterson AFB, Ohio 45433

13. ABSTRACT

The feasibility of stabilizing gas bearing-rotor system by electromagnetic means was investigated analytically. Two devices appeared feasible, namely, a unidirectional device producing a magnetic force to load the bearing without increasing the rotor mass, and an active device producing a controlled electromagnetic force always opposing the motion of the shaft. A numerical example shows that the power loss from using either device together with plain journal bearings compares favorably with tilting-pad gas bearings.

DD FORM 1 NOV 65 1473

Unclassified
Security Classification

Unclassified
Security Classification

14 KEY WORDS	LINK A		LINK B		LINK C	
	ROLE	WT	ROLE	WT	ROLE	WT
Gas Lubricated Bearings						
Electromagnetic Stabilization of Gas Bearings						
Air Bearings, Stabilization						
Gas Bearings, Stabilization						
High Speed Bearing Stabilization						
Instability, Gas Lubricated Bearings						
Stabilization System for Gas Bearings						
Rotor-Bearing Stabilization						
Whirl Suppression - Gas Bearing						
Half Frequency Whirl Suppression						

Unclassified
Security Classification